GEOLOGICA CARPATHICA, FEBRUARY 2016, 67, 1, 83–104 doi: 10.1515/geoca-2016-0005

Cenozoic structural evolution of the southwestern Bükk Mts. and the southern part of the Darnó Deformation Belt (NE Hungary)

ATTILA PETRIK[1], BARBARA BEKE[2], LÁSZLÓ FODOR[2] and RÉKA LUKÁCS[3]

[1]Eötvös University, Department of Physical and Applied Geology, Pázmány Péter sétány 1/C, 1117 Budapest, Hungary; petrik.atus@gmail.com
[2]MTA-ELTE Geological, Geophysical and Space Science Research Group, Hungarian Academy of Sciences at Eötvös University, Pázmány Péter sétány 1/C, 1117 Budapest, Hungary
[3]MTA-ELTE Volcanology Research Group, Pázmány Péter sétány 1/C, 1117 Budapest, Hungary

(Manuscript received May 28, 2015; accepted in revised form October 1, 2015)

Abstract: Extensive structural field observations and seismic interpretation allowed us to delineate 7 deformation phases in the study area for the Cenozoic period. Phase D1 indicates NW–SE compression and perpendicular extension in the Late Oligocene–early Eggenburgian and it was responsible for the development of a wedge-shaped Paleogene sequence in front of north-westward propagating blind reverse faults. D2 is represented by E–W compression and perpendicular extension in the middle Eggenburgian–early Ottnangian. The D1 and D2 phases resulted in the erosion of Paleogene suites on elevated highs. Phase D2 was followed by a counterclockwise rotation, described in earlier publications. When considering the age of sediments deformed by the syn-sedimentary D3 deformation and preliminary geochronological ages of deformed volcanites the time of the first CCW rotation can be shifted slightly younger (~17–16.5 Ma) than previously thought (18.5–17.5 Ma). Another consequence of our new timing is that the extrusional tectonics of the ALCAPA unit, the D2 local phase, could also terminate somewhat later by 1 Myr. D4 shows NE–SW extension in the late Karpatian–Early Badenian creating NW–SE trending normal faults which connected the major NNE–SSW trending sinistral faults. The D5 and D6 phases are late syn-rift deformations indicating E–W extension and NW–SE extension, respectively. D5 indicates syn-sedimentary deformation in the Middle Badenian–early Sarmatian and caused the syn-sedimentary thickening of mid-Miocene suites along NNE–SSW trending transtensional faults. D5 postdates the second CCW rotation which can be bracketed between ~16–15 Ma. This timing is somewhat older than previously considered and is based on new geochronological dates of pyroclastite rocks which were not deformed by this phase. D6 was responsible for further deepening of half-grabens during the Sarmatian. D7 is post-tilt NNW–SSE extension and induced the deposition of the 700 m thick Pannonian wedge between 11.6–8.92 Ma in the southern part of the study area.

Key words: Bükk Mts., Cenozoic, fault pattern, stress field, seismic profile, deformation band.

Introduction

The Darnó Zone is an important NNE-SSW trending structural element located in north-eastern Hungary and reaching the southernmost part of the Slovak Republic (Fig. 1a). The Darnó Fault which is an element of the Darnó Zone is restricted only to the area of Darnó Hill and can be followed up to Bükkszék village. The Darnó Fault is a moderately SE dipping thrust putting the Mesozoic rocks onto Oligocene sediments (Fig. 1b) (Schréter 1951; Telegdi-Róth 1951; Fodor et al. 2005). The western footwall block of the fault is characterized by a gentle monoclinal basin filled with thick Late Oligocene–Early Miocene sequences (Fig. 1b) (Jaskó 1946). The Darnó Line first defined by Pantó (1956) connects the Darnó Fault with Uppony Fault further to the northeast and goes up to the Rudabánya Hills.

The Darnó Deformation Belt (DDB) includes all the NNE–SSW oriented Cenozoic structural elements which extend from the Darnó Fault sensu stricto up to the northwestern margin of the Bükk Mts. (Fig. 2) (Fodor et al. 2005). The Darnó Line and its tectonic influence on Late Oligocene–Early Miocene sedimentation has been recognized for a long time (Báldi 1986; Sztanó & Tari 1993; Sztanó & Józsa 1996) but the tectonic evolution of the southern part of the DDB has been less investigated and understood.

Our research area also includes the southwestern part and foreland of the Bükk Mts. Special emphasis is given to the Felsőtárkány graben (FG) which has a particular structural position while cutting across the Mesozoic rocks (Fig. 2). Our knowledge about the Cenozoic development of the FG is poor and a systematic structural analysis was not carried out although Csontos (1999) and Fodor et al. (2005) briefly described a few major Miocene structures.

The aim of our study is to outline and reveal the Cenozoic structural evolution of the southwestern part of the Bükk Mts. in much more detail than in the previous studies (e.g. Tari 1988; Csontos 1999; Fodor et al. 1999, 2005). We also connect the deformation phases of the Southern Bükk foreland of Petrik et al. (2014) to those of the Darnó Fault sensu stricto. The other objective of our paper is to specify the kinematics and the time of fault activity and reveal new fault indications for the study area in the Cenozoic period.

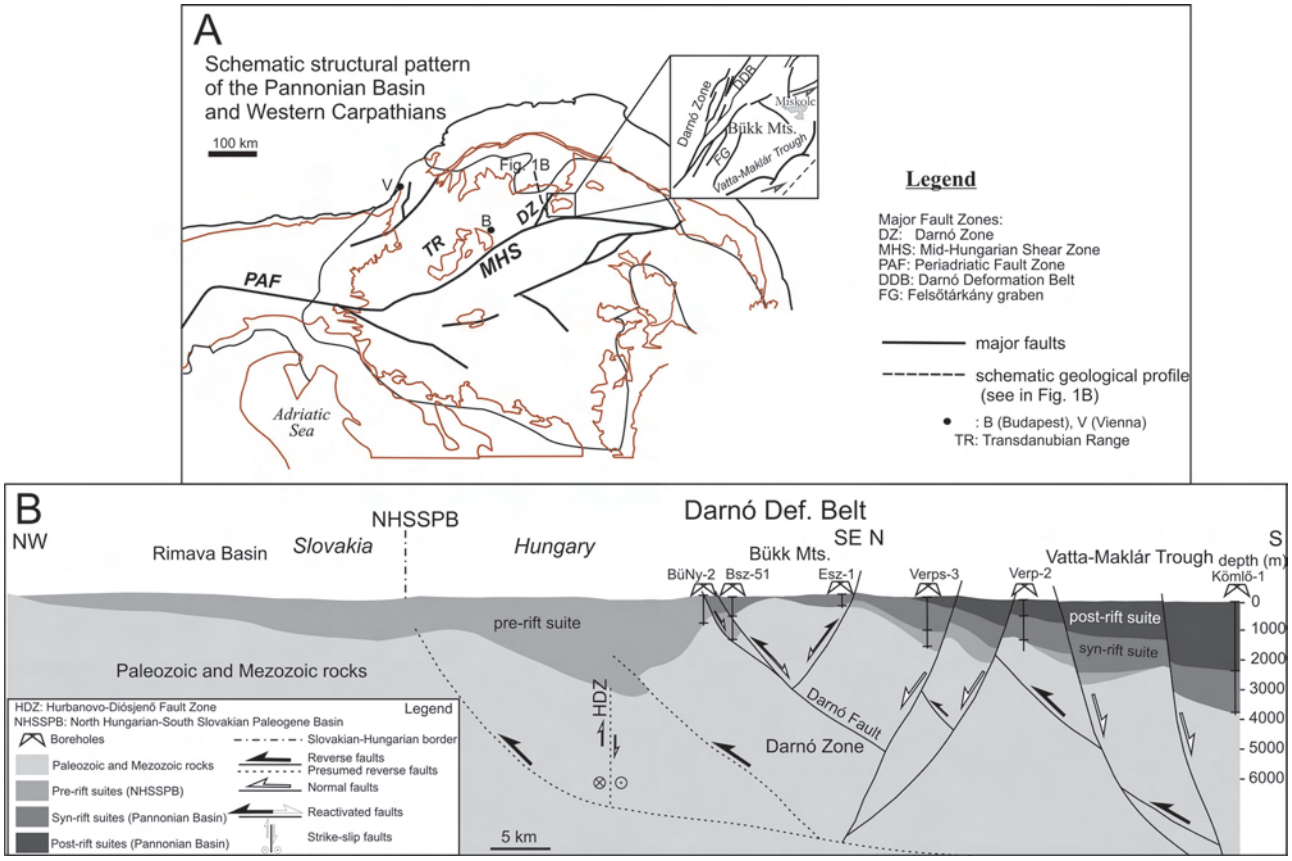

Fig. 1. A — Schematic structural position of the study area within the Carpathians. The inset shows the study area and the Bükk Mts. with its most prominent structures (Fodor 2010). **B** — Schematic geological NNW–SSE oriented cross section indicating the different aged subbasins and their rock piles for the NHSSPB (Petrik et al. 2014). The Slovak part of the NHSSPB drawn after Fusán et al. (1987). Major fault systems are displayed. Note the syn-sediment thickening of Paleogene rocks in front of propagating reverse faults and their pinching out north-westward. Note the normal reactivation of the Darnó Zone. Post-rift rock suites only appear in the Vatta-Maklár Trough. See location of section on Fig. 2.

Methods

A combination of methods was used to understand the tectonic evolution of the area. Our investigation is primarily based on extensive field work covering not only the study area but also the southwestern part of the southern Bükk foreland as well. In this study we present only the most important sites (17 sites, see Table 1) in terms of Cenozoic evolution. We mainly focused on measuring brittle structural elements (faults, joints, deformation bands) in rocks with different Cenozoic ages.

We calculated stress tensors from slickenside lineations on fault planes using Tector 1994 software with the algorithm described by Angelier (1984, 1990). This software determines the reduced stress tensor including the position of the three principal stress axes and their relative magnitude ($\Phi=\sigma_2-\sigma_3/\sigma_1-\sigma_3$). The Φ value ranges from 0 to 1 depending on the stress state that acted on the fault planes. The principal stress axes (σ_1, σ_2, σ_3) are orthogonal to each other and the resolved shear stress perpendicular to them is zero. σ_1, σ_2, σ_3 indicate the maximum, the intermediate and the minimum compression direction, respectively. When sufficient data was available we used automatic phase separation often combined with manual separation (Angelier & Manoussis 1980). During stress tensor calculation we took into account the average misfit angle (α) between measured striae and the calculated shear stress (τ) (ANG criterion) and the misfit between the direction and size of a maximum calculated shear vector and the unit vector along the striae (RUP criterion) (Angelier 1984, 1990). We accepted a fault was part of a stress field when these parameters were below 22.5° and 45 %, respectively. Based on Anderson's assumption (Anderson 1951) we estimated the main stress axes for faults without striae and joints.

Backtilting of measured structures was also applied to reveal whether the deformation might have taken place before,

Fig. 2. Simplified geological map of the study area with the position of investigated sites, important boreholes, seismic profile and geological cross sections. Note the dominance of NE–SW trending faults which were modified with respect to original base maps of Less et al. 2005.

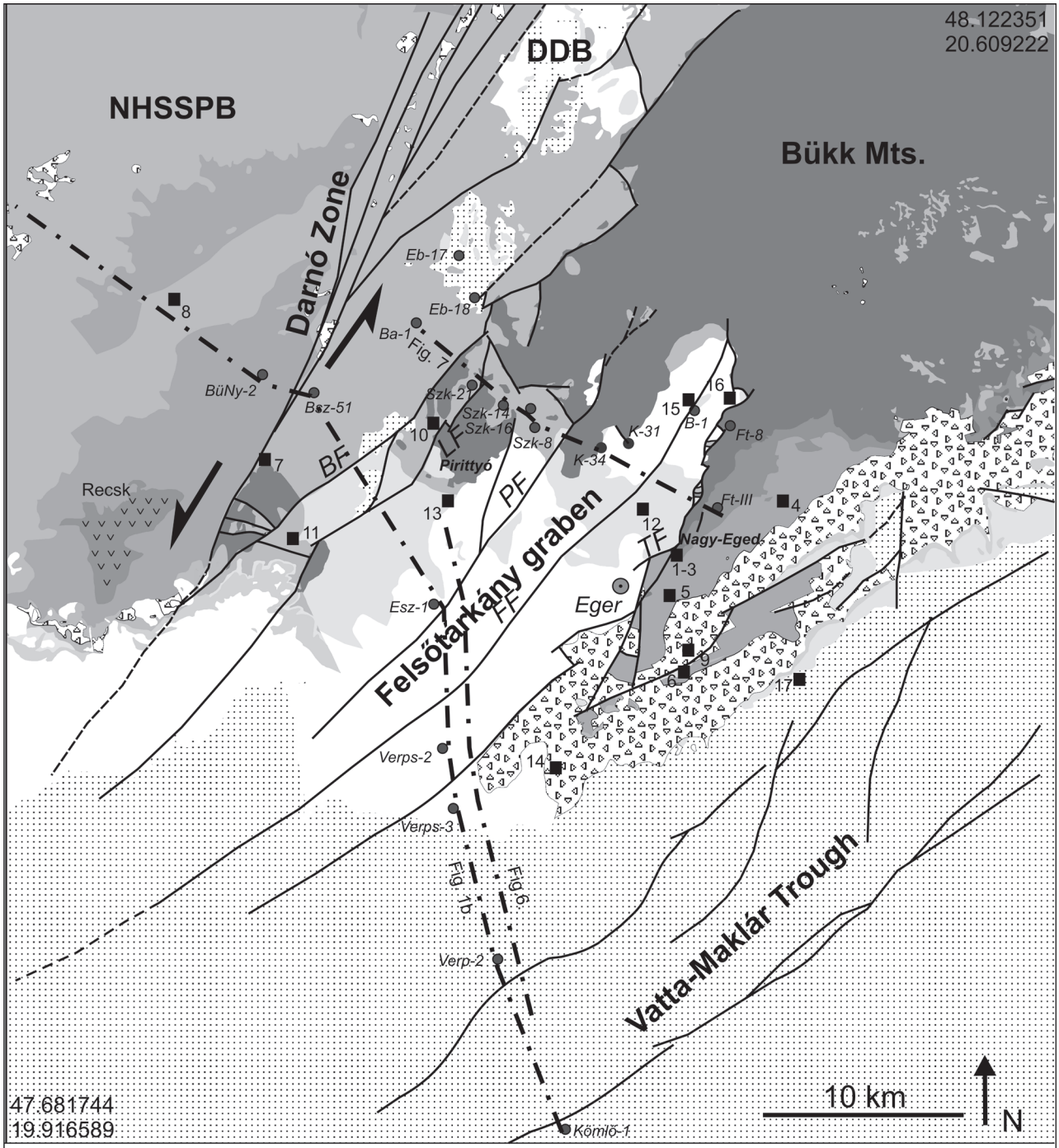

■ **Investigated sites**
1-3. Kis-Eged
4. Noszvaj
5. Eger, Wind
6. Andornaktálya
7. Kis-Hill
8. Pétervására
9. Eger, Tihamér
10. Bátor
11. Sirok
12. Felnémet
13. Egerbakta
14. Demjén
15. Felsőtárkány
16. Bambara
17. Novaj

TF: Tárkány Fault
FF: Felnémet Fault
PF: Pirittyó Fault
LF: Laskó Fault
BF: Bátor Fault

DDB: Darnó Deformation Belt
NHSSPB: North Hungarian South Slovakian Paleogene Basin

● Major boreholes
⊙ Town
Major faults
Major strike-slip faults
Uncertain faults
Profiles (seismic and geological)

Late Miocene
Middle Miocene
„upper volcanoclastic unit"
„middle volcanoclastic unit"
„lower volcanoclastic unit"
Early Miocene
Oligocene volcanites
Oligocene
Eocene
Paleozoic and Mesozoic

Table 1: The investigated sites with their geographical coordinates and the number of measured data.

Sites	X coord. (lat.)	Y coord. (long.)	Number of data
1. Kis-Eged (Triassic)	47.91892	20.40772	26
2. Kis-Eged (Eocene)	47.91514	20.40777	10
3. Kis-Eged (Oligocene)	47.91618	20.41052	23
4. Noszvaj (Oligocene)	47.93634	20.46443	18
5. Eger, Wind (Oligocene)	47.89863	20.40075	26
6. Andornaktálya (Oligocene)	47.86966	20.40888	16
7. Kis-Hill (Eggenburgian)	47.95060	20.15334	33
8. Pétervására (Eggenburgian)	48.02101	20.09856	22
9. Eger, Tihamér (Ottnangian)	47.87909	20.40395	11
10. Bátor (Ottnangian–Karpatian)	47.96782	20.26044	34
11. Sirok (Early Badenian)	47.92972	20.19362	17
12. Felnémet (Middle Badenian)	47.93365	20.38435	39
13. Egerbakta (Middle Badenian)	47.94082	20.29232	12
14. Demjén (Middle Badenian)	47.83465	20.34455	41
15. Ftárkány (Sarmatian)	47.97711	20.41543	22
16. Bambara (Sarmatian)	47.97640	20.43542	10
17. Novaj (Pannonian)	47.86708	20.47287	8

during or after a specific tilting event in order to determine the relative chronology among stress fields. We took into account the average dips of Eocene, Oligocene and Miocene volcanoclastic levels. We made two scenarios for tilting of beds because dip data show spatial variations even if measured from the same stratigraphic horizons; one of them supposes a more significant tilting (altogether 35˚ for the Eocene) and a more moderate scenario (altogether 25˚ for the Eocene).

Syn-sedimentary deformations allowed us to delineate the structural phases more precisely. Deformation bands were also important, while they could form closely after sedimentation or only much later. The prevailing deformation mechanism in these bands refers to the host rock porosity and its state of consolidation which is irreversibly changing over time. Consequently, the differences in deformation mechanism within generations of bands give us relative chronology between them based on subsidence history. Thin sections were made from each deformation band to examine their deformation mechanism. We analysed and compared them under a light microscope. The differences in deformation mechanism within generations of bands gave us a relative chronology between them based on subsidence history. Finally, each deformation band was integrated into the structural phases of the study area.

Some 2D reflection seismic profiles located south of the study area were also investigated to better understand the subsurface structures. Geological profiles were constructed by using borehole data and our structural observations. The faults on seismic profiles have been correlated with their counterparts on geological profiles. Using combinations of these methods we produced schematic sequential structural cartoons depicting the main Cenozoic fault systems.

Geological background

The study area includes the southern part of the Darnó Deformation Belt and the southwestern part of the Bükk Mts. (NE Hungary) (Fig. 2). Mesozoic deposits representing different nappes are composed of Triassic carbonates, Middle Triassic volcanoclastic rocks and Jurassic siliciclastic sequences with Middle Jurassic basalt suites and radiolarite (Fig. 3). These rocks were folded into NE–SW trending anticlines and synclines during or after Late Jurassic–Early Cretaceous nappe stacking (Csontos 1999). The Paleogene history of the study area is strongly tied to the evolution of the North Hungarian-South Slovakian Paleogene Basin (NHSSPB) which is interpreted as a flexural basin situating in a retroarc position with respect to the Western Carpathian orogenic arc (Tari et al. 1993). The beginning of the basin formation is marked by an uppermost Eocene transgressive sequence including terrestrial to shallow-marine clastics and limestone (Báldi & Báldi-Beke 1985; Nagymarosy 1990). The average dip of the Eocene rocks varies between 25˚ and 35˚ but locally can reach 45˚. Due to tectonic subsidence they were covered by shallow bathyal marls, laminated claystone and thick siltstone of Early Oligocene age (Fig. 3) (Báldi 1986; Less 2005). The average dip of Oligocene deposits ranges from 15˚ to 25˚. The last phase in basin evolution is represented by Late Oligocene to earliest Miocene (Eggenburgian) fine- to medium-grained clastics west of the Darnó Fault. However, the Miocene part seems to be missing in the study area due to the "Intra-Egerian" denudation which was the result of tectonic uplift and/or the TB1.3 eustatic cycle (Báldi & Sztanó 2000). The first major tilting (I. Tilting) can be attributed to this denudation in the earliest Miocene time (Fig. 3). Sedimentation was influenced by eustatic sea level changes and in a minor way by local fault activity (Sztanó & Tari 1993; Báldi & Sztanó 2000). The largest such fault in the study area, the Darnó fault acted as a SE-dipping reverse fault creating a deep flexural sub-basin (Fig. 1b, Sztanó & Tari 1993; Tari et al. 1993; Fodor et al. 2005). In the study area, the Lower Miocene rock suites are mainly confined to the Darnó Zone where a small fault-controlled fan-delta (Darnó Conglomerate) was deposited at the eastern margin of NHSSPB (Fig. 3) (Sztanó & Józsa 1996). The age of this conglomerate is well constrained by radiometric and biostratigraphic data indicating ~21.4–20.9 Ma (Less et al. 2015). In the southern Bükk foreland correlative sediments were not proved unequivocally, or alternatively, if present, they are represented by continental variegated clay, conglomerate (Less 2005).

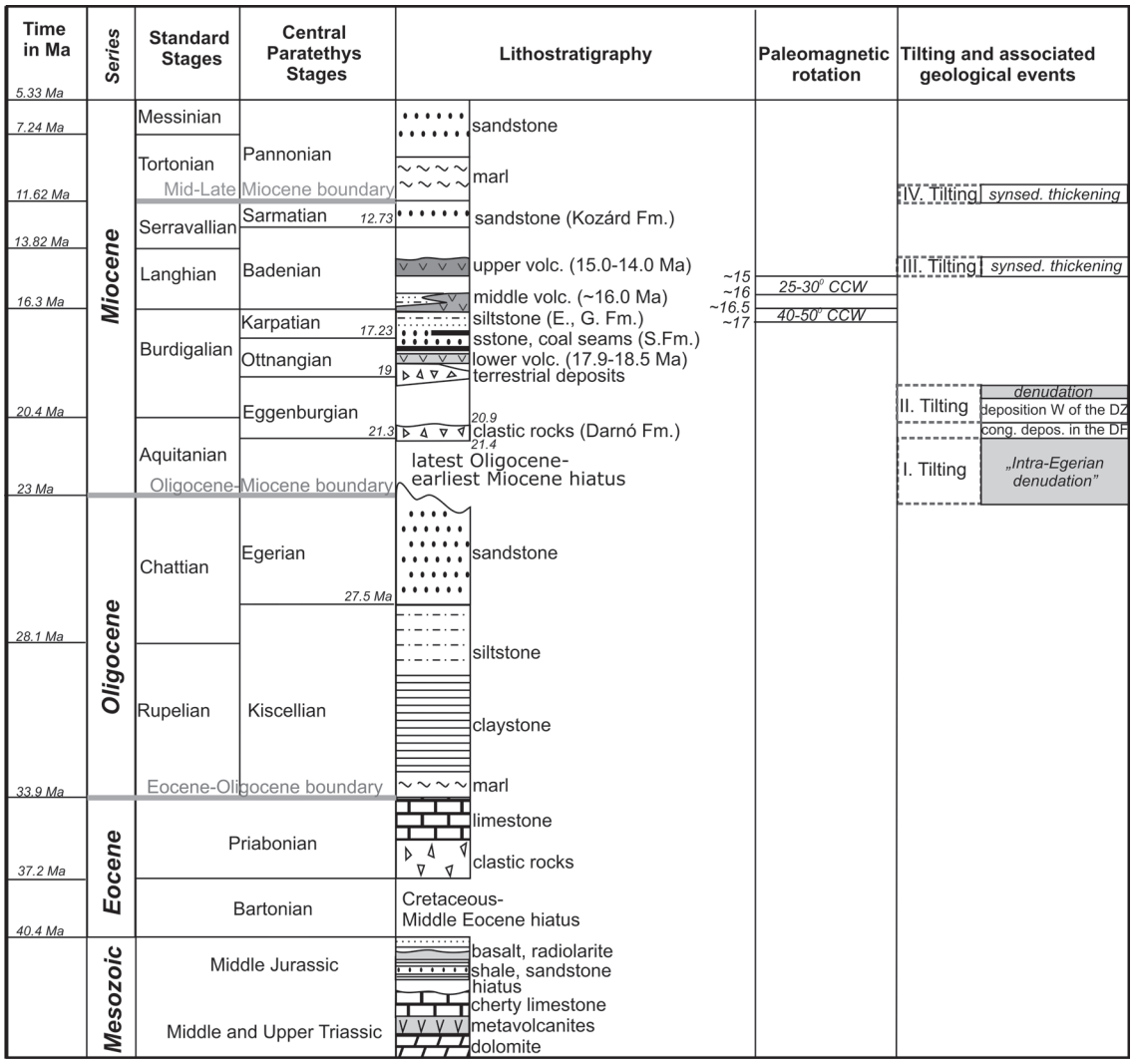

Fig. 3. Lithostratigraphic chart of the study area. Standard stages and their absolute ages are based on Lourens et al. (2004). Central Paratethys stages and their absolute ages are based on Hohenegger et al. (2009); Popov et al. (1993); Steininger et al. (1996). The U/Pb radiometric ages of volcanoclastic levels are taken from Lukács et al. (2014a,b). The Sr-age of Darnó Fm. is taken from Less et al. (2015). Note that the Mesozoic is not time proportional. Major tilting events and associated geological events are also demonstrated. **DZ** — Darnó Zone, **DF** — Darnó Fault.

The evolution of the NHSSPB was terminated by a regional unconformity and denudation associated with a second tilting event (II. Tilting) in the middle part of the Early Miocene, ca. 20–19 Ma ago. Paleogene sediments outcrop exclusively on the eastern margin of the FG due to the earliest Miocene and Mid-Late Miocene erosional events (Fig. 2).

During the Early Miocene the NHSSPB was dextrally displaced from its original continuation, from the North Slovenian Paleogene Basin by the combined Periadriatic-Balaton Fault system (PAF) (Kázmér & Kovács 1985; Báldi 1986; Csontos et al. 1992; Fodor et al. 1998). Post-19 Ma evolution was part of the formation and evolution of the extensional Pannonian Basin system (Royden & Horváth 1988). The rock suites in the Pannonian Basin are divided into pre-rift, syn-rift and post-rift sediments and volcanites. Extensive rhyolitic and dacitic pyroclastic rocks were produced by many explosive eruptions of late Early to Mid-Miocene times in the Pannonian Basin (e.g. Szabó et al. 1992). These volcanic rocks are exposed exceptionally well in the southern Bükk foreland and can give radiometric age constraints on the Miocene stratigraphy and geodynamic evolution of the area (Márton & Pécskay 1998; Póka et al. 1998; Szakács et al. 1998; Harangi et al. 2005; Lukács et al. 2005, 2007, 2009; Pentelényi 2005). New U-Pb ages on zircons of the pyroclastic units in the Bükk foreland indicate that the oldest pyroclastic unit ("lower unit") is somewhat younger (~18.5–17.9 Ma; Lukács et al. 2014a,b), than previously suggested (21–18.5 Ma; Márton & Pécskay 1998), the "middle volcanoclastic level" is restricted to ca. 16 Ma (Lukács et al. 2014a,b) in contrast to the former suggestion of between 17.5–16,0 Ma (Márton & Pécskay 1998), while the "upper" volcanoclastic level involves several units, spanning broadly from 15 to 14 Ma (Lukács et al. 2015).

In our study area the "lower" and "middle" pyroclastic rocks can be found sporadically, preserved in karstic depressions (Hartai 1983; Pelikán 2005). In the Southern Bükk

foreland, the pyroclastic rocks can be found in NE–SW trending stripes (Fig. 2) (Pentelényi 2005; Less et al. 2005). Some boreholes north-east and north-west of the Bükk Mts. revealed that the lower rhyolitic tuff is covered by an Ottnangian–Karpatian fluviatile-paludal sequence including several coal seams (Salgótarján Fm., Pelikán 2005). The coal seams tend to be paralic in the upper part and are often intercalated by sandstone and sandy silt indicating a normal salinity environment (Ádám 2006; Püspöki et al. 2009). The relationship between the volcanic rocks and sedimentary formations (Pelikán 2005), and the new preliminary U-Pb ages (Lukács et al. 2014a,b; Lukács et al. 2015) indicate that the coal-bearing sequence is younger, and could involve only the upper Ottnangian (ca. 18 Ma) and Karpatian. This formation appears on the surface west of the FG where several boreholes (Szk-6, Szk-8) encountered it unconformably overlying Mesozoic rocks (Fig. 2). The deposition of the Salgótarján Fm. partly overlaps with the Karpatian basal conglomerate and sandstone which was deposited on a coastal plain (Egyházasgerge Fm.) (Fig. 3) (Pelikán 2005). This sediment crops out at the north-western margin of the FG where it overlies unconformably the Mesozoic rocks and consists of a transgressive sequence containing Mesozoic limestone and dolomite pebbles (Fig. 2) (Pelikán 2005). At the south-eastern margin of the FG some patches of Karpatian sediments were also mapped (Fig. 2). Closer to the Darnó Fault this formation is overlain by Karpatian shallow bathyal siltstone (Fig. 3) interbedded by sandstone layers (Garáb Fm.) (Pelikán 2005). This formation is restricted to the westernmost part of the study area where its thickness varies between 100–150 m. The Early Badenian sediments and middle volcanoclastic rocks are found sporadically in the DDB area in the vicinity of Szilvásvárad (Pelikán 2005). The upper volcanoclastic level appears on the surface in the FG and further to the west with variable thickness (~50–150 m) (Fig. 2). It tends to be pinched out in a westward direction close to the Darnó Line. Some boreholes (Verps-3, 4), southwest of the study area revealed more than 500 m thick pyroclastic rocks of Badenian and Sarmatian age in the hanging-wall block of a major NE–SW trending transtensional fault. The wedge-shaped syn-sedimentary thickening of these rocks in the tilted blocks was associated with the third major tilting event (Fig. 3). These rocks can be the temporal equivalent of the middle and upper volcanic level. In the FG the upper volcanoclastic rocks are overlain by shallow marine/nearshore sandstone, tuffitic sandstone (Kozárd Fm.) with Sarmatian vertebrates (Fig. 3) (Kessler & Hír 2012). The thickness of the Sarmatian rocks is variable in the Felsőtárkány graben, but in the Southern Bükk foreland, in the hanging-wall blocks of normal faults it can reach 500 m (Pelikán 2005).

For a long time, the Late Miocene sedimentation was considered post-rift, but new structural data demonstrate ongoing faulting at least up to 8 Ma in the study area (Petrik et al. 2014) and in the whole Pannonian basin (Fodor et al. 2013). The thick Late Miocene (Pannonian in local terms) sedimentary unit consists of lacustrine marlstone, followed by basin floor sandy turbidites, clayey slope deposits, sandy deltaic and variegated fluvial suites (Magyar et al. 1999, Sztanó et al. 2013). The second major tilting occurred during the beginning of this sedimentation, in the early Late Miocene and was accompanied by syn-tectonic thickening of the early Pannonian sediment pile, particularly the formations below the slope unit (Petrik et al. 2014). This thickening can be associated with the fourth major tilting event of the area (Fig. 3). In the FG and in the southern Darnó DB Pannonian sediments are missing on the surface and were only preserved in the syn-sedimentary NE–SW trending Vatta-Maklár Trough south of the study area (Tari 1988; Petrik et al. 2014). This distribution is due to the post-Pannonian erosion induced by neotectonic (Quaternary) uplift of the Bükk Mts. and their margins (Dunkl et al. 1994). This uplift was accompanied by very modest post-sedimentary tilting which can be estimated from the dip degree of the uppermost imaged Late Miocene horizons to be 1–2°.

The most relevant structures of the DDB are the NNE–SSW trending normal faults (Fig. 2). These faults are responsible for sudden thickness changes within the Miocene sequences. The NNE–SSW trending faults are connected to the NE–SW trending major faults of the Vatta-Maklár Trough (Fig. 2). We will discuss the geometry and kinematics and age of these faults in the successive chapters.

Results

Main structural phases

The Cenozoic structural evolution history of the study area can be divided into 3 main separate periods on the basis of the fault kinematics, the time of fault activity and their influence on sedimentation.

Pre-rift deformations

D1 phase (Eocene? – early Eggenburgian)

This deformation is characterized by NW–SE compression and perpendicular extension but small deviation in σ_1 direction can be observed (Fig. 4, sites 1, 2, 3, 5, 6, 7). The D1 phase was observed in Upper Eocene to Oligocene rocks and Eggenburgian conglomerate of the Darnó Fm.

The NE–SW trending conjugate reverse faults and oblique dextral strike slip faults are the main structures of this deformation phase (Fig. 4). Small scale (~5 cms) reverse offsets and folds with NE–SW trending axes can be associated with this phase. In site 5 (Fig. 4), NW–SE trending dilational

Fig. 4. The summary table of stress fields and main deformation phases. RUP (in %), ANG (in degree) criteria and phi value are indicated for stress tensor calculation. After the value of criteria, the number of unfitted data is also displayed. The structural data of site 8 were measured by L. Fodor and F. Bergerat (Paris).

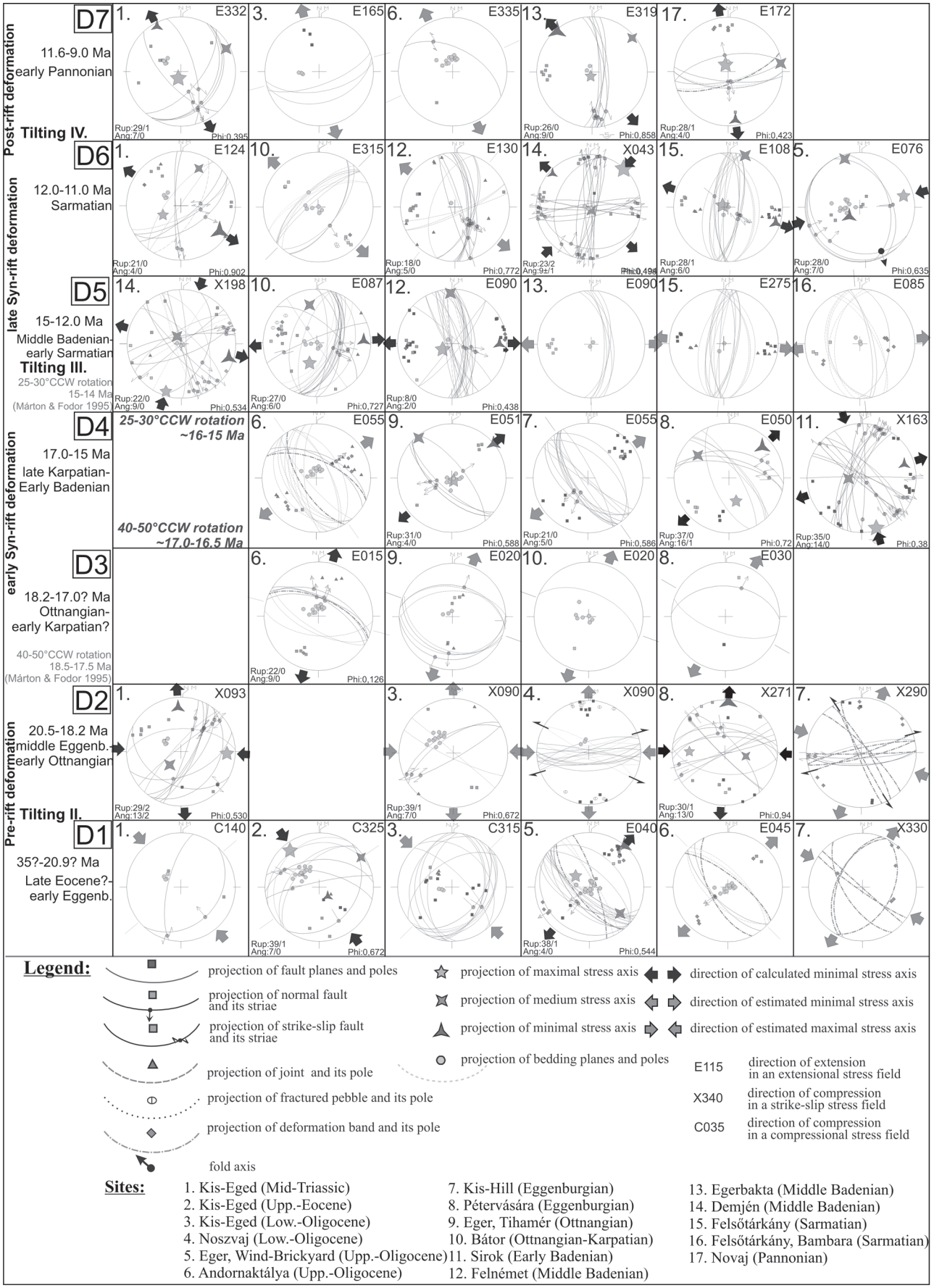
Post-rift deformation
late Syn-rift deformation
early Syn-rift deformation
Pre-rift deformation
D7
11.6-9.0 Ma
early Pannonian
Tilting IV.
D6
12.0-11.0 Ma
Sarmatian
D5
15-12.0 Ma
Middle Badenian-
early Sarmatian
Tilting III.
25-30°CCW rotation
15-14 Ma
(Márton & Fodor 1995)
D4
17.0-15 Ma
late Karpatian-
Early Badenian
25-30°CCW rotation
~16-15 Ma
40-50°CCW rotation
~17.0-16.5 Ma
D3
18.2-17.0? Ma
Ottnangian-
early Karpatian?
40-50°CCW rotation
18.5-17.5 Ma
(Márton & Fodor 1995)
D2
20.5-18.2 Ma
middle Eggenb.-
early Ottnangian
Tilting II.
D1
35?-20.9? Ma
Late Eocene?-
early Eggenb.
Legend:
projection of fault planes and poles
projection of normal fault and its striae
projection of strike-slip fault and its striae
projection of joint and its pole
projection of fractured pebble and its pole
projection of deformation band and its pole
fold axis
projection of maximal stress axis
projection of medium stress axis
projection of minimal stress axis
projection of bedding planes and poles
direction of calculated minimal stress axis
direction of estimated minimal stress axis
direction of estimated maximal stress axis
E115 direction of extension in an extensional stress field
X340 direction of compression in a strike-slip stress field
C035 direction of compression in a compressional stress field
Sites:
1. Kis-Eged (Mid-Triassic)
2. Kis-Eged (Upp.-Eocene)
3. Kis-Eged (Low.-Oligocene)
4. Noszvaj (Low.-Oligocene)
5. Eger, Wind-Brickyard (Upp.-Oligocene)
6. Andornaktálya (Upp.-Oligocene)
7. Kis-Hill (Eggenburgian)
8. Pétervására (Eggenburgian)
9. Eger, Tihamér (Ottnangian)
10. Bátor (Ottnangian-Karpatian)
11. Sirok (Early Badenian)
12. Felnémet (Middle Badenian)
13. Egerbakta (Middle Badenian)
14. Demjén (Middle Badenian)
15. Felsőtárkány (Sarmatian)
16. Felsőtárkány, Bambara (Sarmatian)
17. Novaj (Pannonian)

band filled with syntectonic sediment matrix clearly indicates NE–SW extension during Late Oligocene sedimentation (Petrik et al. 2014).

NW–SE trending deformation bands in Eggenburgian conglomerate are related to this phase and indicate NE–SW extensional deformation. These bands show a disaggregation type deformation mechanism and indicate early deformation which can be attributed to a stress field which occurred soon after sedimentation. Another argument of the earliest timing of these bands is two sets of relative chronological criteria. The NW-SE striking bands are slightly reversely displaced by a set of NE–SW trending deformation bands (Fig. 5a). These bands can belong to the earliest deformation phase due to their strikes which perfectly fit into the D1 phase. The disaggregation type deformation mechanism also supports early deformation at a shallow depth (<1 km) (Fossen 2007). On the other hand the following deformation structures (third in relative order) suggest more consolidated host rock where calcite-infilled lenses as a marker of displacement are already present along the bands. This observation shows a transitional character from deformation bands toward discrete faults and belongs to the following D2 phase (Fig. 5b,c).

The structures belonging to this phase might predate the second major tilting event (ca. 20–19 Ma) proven by the backtilting test (Petrik et al. 2014).

On NW–SE trending seismic profiles some NW-vergent blind reverse faults can be presumed resulting in folding and wedge-shaped thickening of Paleogene sediments (Fig. 6). North-westward the Paleogene sediments are thinning and pinching out on the flank of an elevated high. Some small-scale SE-vergent backthrusts were often associated with propagating reverse faults (below Verp-3 borehole, Fig. 6). Above some blind reverse faults the Mesozoic rocks are directly overlain by Early to Mid-Miocene pyroclastic rocks (Verp-2, Esz-1 boreholes). Paleogene sediments are missing on these elevated highs due to either or both the earliest Miocene erosion or original non-deposition. In the FG area the Paleogene rocks only crop out in the south-eastern part of the Nagy-Eged Hill (Fig. 2). If we project the subsurface architecture of sediments and faults of seismic profiles into the area of the FG, similar wedge-shaped Paleogene sediments can be presumed below the Mid-Miocene tuffs and sandstone (Fig. 7). In this case the precursor basin of the FG would be bounded by NW-vergent blind reverse faults on its eastern side. From the western margin of the FG Paleogene sediments are missing as proven by boreholes which reached Mid-Miocene sediments directly above Mesozoic rocks (K-31, K-34 boreholes) (Figs. 2, 7).

Thickening of Paleogene sediments in front of the propagating reverse faults along with syn-sedimentary dilational bands in late Oligocene sandstone suggest that the age of the D1 phase can be put into Late Oligocene time, although an Early Oligocene onset cannot be ruled out. However, deformation bands in site 7 (Figs. 2, 4) allow us to extend the upper time limit of the D1 phase into the early Eggenburgian.

D2 phase (middle Eggenburgian–early Ottnangian)

This deformation is represented by E–W compression and perpendicular extension (Fig. 4, sites 1, 3, 4, 7, 8). This phase has dominantly strike-slip character with NW–SE trending sinistral and NE–SW trending dextral strike-slip faults. This deformation affected siliciclastic rocks with ages ranging from Late Oligocene to Eggenburgian. The lower volcanoclastic unit was not involved in this deformation. Fractured pebbles in Upper Oligocene conglomerate indicate syndiagenetic deformation because fractures could not be traced in the matrix (Fig. 4, site 5). Some conjugate NE–SW dextral and NW–SE trending sinistral cataclastic deformation bands in Eggenburgian conglomerate were also attributed to this phase (Fig. 4, site 7). This D2 phase postdates or/and partially overlaps with the second major tilting.

On seismic profiles Eggenburgian rocks are identified based on their distinct seismic character from the overlying volcanoclastic units (Fig. 6). They are found in front of blind reverse faults and are displaced in both reverse and normal ways indicating strike-slip deformation. In the hanging-wall block of major reverse faults the top of the Oligocene is

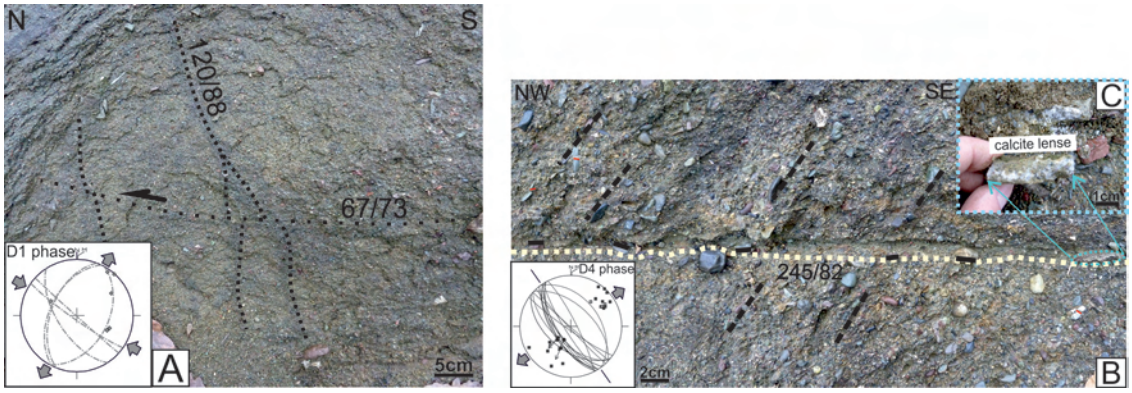

Fig. 5. Outcrop-scale structures at site 7 (Figs. 1, 4), just near the Darnó Fault. In photo **A** deformation bands (black dotted lines) are represented by sets of anastomosing structures which are darker than the host sandstone. One set of bands are thicker (1–1.5 cm) and crosscut by thinner (0.3–0.5 cm) apparently reverse bands, which gives their relative chronology. In photo **B**, viewed from above, the deformation band is an almost 1 cm thick visibly finer grained zone with negative relief (white dashed line), in which the main clasts are reoriented parallel to the band (black lines) and generally contain small calcite lenses (photo **C**) indicating transitional stage to faults. Sedimentary bedding is marked by black dashed lines.

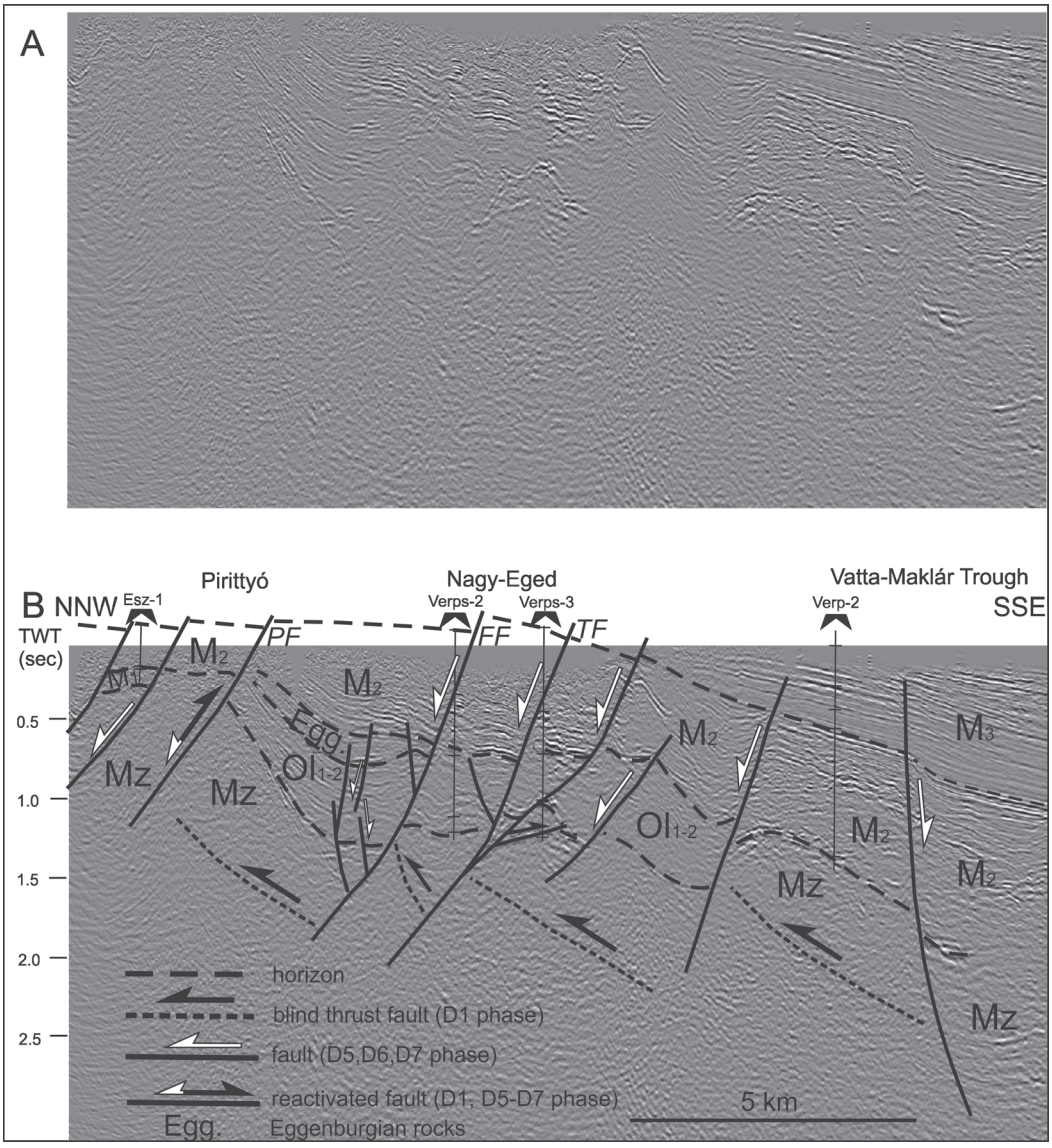

Fig. 6. Uninterpreted **(A)** and interpreted seismic profiles **(B)** of the study area completed after Petrik et al. 2014. For the location of the seismic profile, see Fig. 2. Note the blind reverse faults of the D1 phase. Normal faults dipping NW belong to the D5-D7 phases.

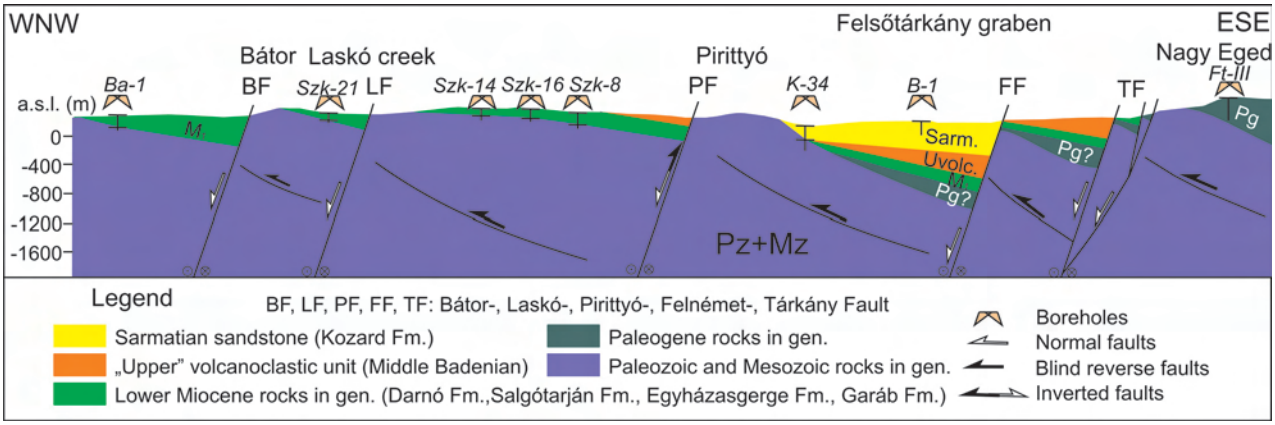

Fig. 7. WNW–ESE oriented geological cross section of the study area with the important boreholes and geographical localities. Note the presumed blind reverse faults of the D1 phase and the majority of WNW dipping normal faults of phases D5–D6. Note the pinching out of the Paleogene in the north-westward direction. The Felsőtárkány graben is interpreted as a Mid-Miocene half-graben.

eroded and covered by Mid Miocene volcanoclastic suites (Fig. 6). This erosion or original non-deposition might be tied to both the first and second major tilting events during the earliest Miocene.

At the southern elevated highs of the Vatta-Maklár Trough the Late Oligocene was also eroded and covered by Early-Mid-Miocene volcanoclastic rocks as biostratigraphic data prove (Majzon 1961). North of these elevated highs several hundred metres of poorly dated terrestrial suites with conglomerate levels were drilled below the lower volcanoclastic level in the Vatta-Maklár Trough.

The conjugate deformation bands in Eggenburgian conglomerate indicates post-tilt deformation as opposed to those belonging to the D1 phase. The structures belonging to D2 show post- or partially syn-tilt deformation with respect to a second major tilting which took place ca. 20–19 Ma. D3 deformation was not observed in the lower volcanoclastic units therefore the upper age limit is ~18.5–17.9 Ma indicated by new zircon U-Pb age results (Lukács et al. 2014a,b).

Syn-rift deformations

All syn-rift phases indicate pre-tilt deformation with respect to the early Late Miocene tilting event proven by positive back-tilt tests (Fig. 4).

Early syn-rift phase (D3, late Ottnangian–early Karpatian)

This deformation is characterized by NNE–SSW extension (Fig. 4., sites 6, 8, 9, 10). D3 is very similar to D2 in terms of extensional direction but this stress field is exclusively represented by extensional structures. This deformation was observed in rocks with ages ranging from Late Oligocene to early Karpatian. The lower volcanoclastic unit was already involved in this deformation.

Conjugate WNW–ESE trending normal faults clearly indicate NNE–SSW extension. Some conjugate weakly cataclastic deformation bands forming in the still poorly consolidated Upper Oligocene sandstone also show a similar extensional direction. In Ottnangian-Karpatian sandstone (Salgótarján Fm.) we observed syn-sedimentary deformation along a WNW–ESE trending normal fault (Fig. 8a). Along the fault some layers accommodate the deformation by folding while others indicate 2–3 cm normal offset; this behaviour is due to the competence contrast. In the hanging wall block, the equivalent layers show small-scale thickening. Downward along the fault a thick silty layer forms an extensional monocline without displacement (Fig. 8a). This structure may indicate a long-segmented normal fault. A few covered normal faults in the Ottnangian lower volcanoclastic suite also indicate syn-sedimentary NNE–SSW extension at that time (Fig. 8b). Along these WNW–ESE oriented normal faults 10–15 cm offsets were observed.

The age of this stress field is Ottnangian-early Karpatian constrained by syn-sedimentary deformation structures, and also by the possible timing of the subsequent rotational deformation (see Fig. 3).

Paleomagnetic measurements from lower volcanoclastic suites indicate 45–50° CCW rotation (Márton 1990; Márton & Pécskay 1998). The first CCW rotation was bracketed between 18.5–17.5 Ma (Márton & Márton 1996; Márton & Pécskay 1998). Fodor (2010) was the first to establish NNE–SSW extension as a first sign of the Pannonian rifting. This

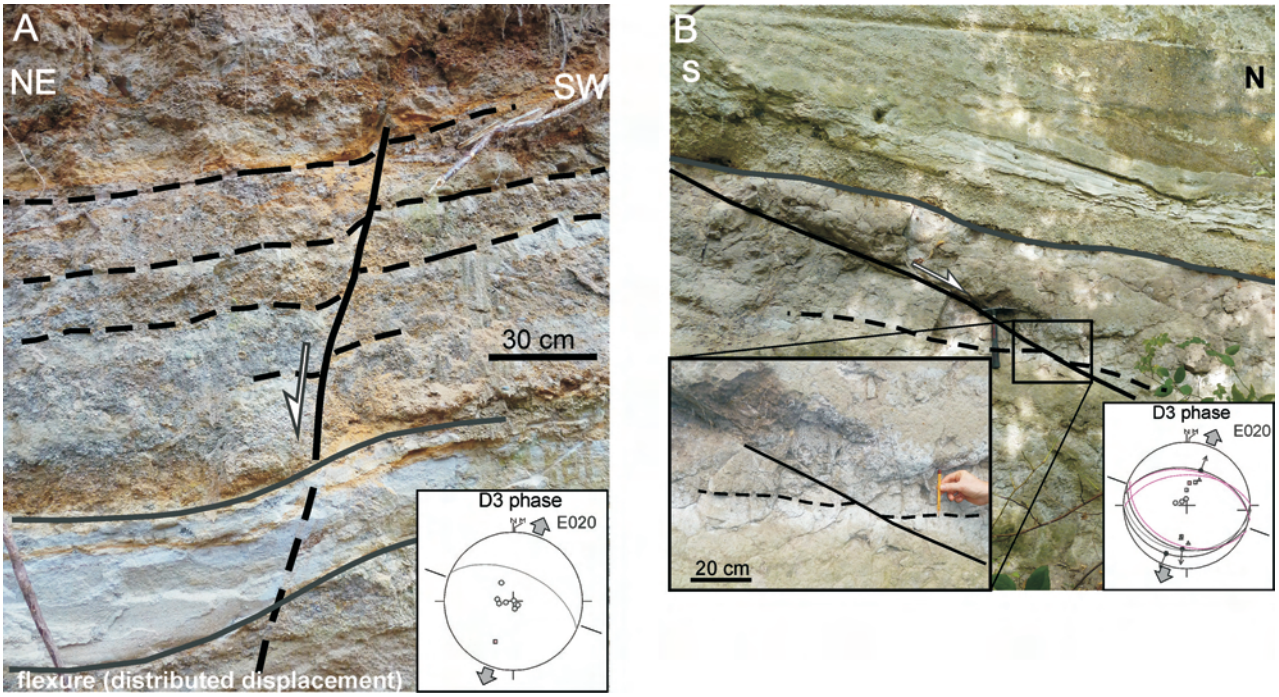

Fig. 8. A — The syn-sedimentary WNW–ESE trending normal faults in site 10. Across the fault some layers accommodate the deformation by folding while others indicate 2-3 cm normal offset. Downward along the fault an extensional monocline developed in a thick silty layer. **B** — Covered faults in lower volcanoclastic units in site 9. Along the normal faults 10–15 cm displacement can be seen.

phase should predate the first CCW rotation because of the good correlation between paleomagnetic data and apparent stress axes rotations (Fodor 2010). He placed this rotation in the Ottnangian. Our observation on syn-sedimentary or covered faults may suggest that the first CCW rotation seems to be slightly younger than previously thought and can probably be placed within the Karpatian (Fig. 3). The exact timing depends on the age of volcanoclastics and the age of site 10.

D4 phase (late Karpatian-Early Badenian)

The D4 phase is demonstrated by NE–SW extension (Fig. 4, sites 6, 7, 8, 9, 11). Sediments correlative to this deformation phase are preserved in the western margin of the DDB and the Felsőtárkány graben (FG). NW–SE trending conjugate normal deformation band faults with calcite-infilled lenses (Fig. 5b,c) belong to this phase. Some oblique dextral faults of pre-existing WNW–ESE oriented normal faults indicate post-D3 deformation (site 8, Fig. 4). The D4 phase already affected the Early Badenian rocks in Sirok (site 11, Fig. 4) where NNE–SSW trending sinistral and NW–SE trending dextral strike-slip faults were identified by Bergerat et al. (1984) and again by Fodor et al. (2005). This is the reason why we postulate that the dominant extension may have been accompanied by strike-slip deformation.

Márton & Fodor (1995) and Fodor et al. (1999) suggested that the D4 extension can be bracketed between the first and second phase of rotation in NE Hungary. Accepting this idea, this D4 phase can be placed in the latest Karpatian to Early Badenian.

Late syn-rift deformations

D5 phase (Middle Badenian–early Sarmatian)

This phase is one of the most represented structural phases in the study area and it is characterized by E–W extension (Fig. 4, sites 10, 12, 13, 14, 15, 16). The D5 phase includes N–S to NNE–SSW trending conjugate normal faults and deformation bands (Figs. 9, 10). N–S trending conjugate deformation bands in Sarmatian sandstone (in site 16) crosscut each other and indicate E–W extension (Fig. 10). NW–SE dextral and NE–SW sinistral conjugate strike-slip faults along with cataclastic type deformation bands with similar orientations are also common in the study area (Fig. 4, site 14) and also in the Southern Bükk foreland (Fig. 4). NW–SE oriented normal faults of the D4 phase were reactivated as oblique dextral faults during the D5 phase.

We investigated several sites in the FG area where the upper volcanoclastic units and early Sarmatian sandstones outcrop (Fig. 4, sites 12, 15, 16). The D5 phase was present in all of these sites and always indicated the oldest deformational event. A covered normal fault indicating syn-sedimentary E–W extension in Sarmatian tuffitic sandstone is also part of this D5 phase (Fig. 9). Along this antilistric normal fault a syntectonic sediment wedge was formed. Close to the antilistric fault the gently tilted layers become folded due to fault drag or they form an extensional monocline above the upward propagating normal fault (Fig. 9). The upper part of this wedge is a well-seen discordance surface above which the layers are mainly sub-horizontal and cover the upward continuation of the fault. An impressive N–S trending normal fault was observed in the upper volcanoclastic unit resulting in 50 cm displacement of a pyroclastic channel. Along this fault multiple oblique dextral-normal striations

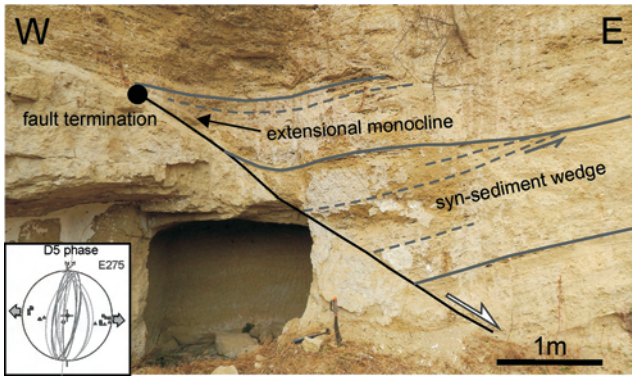

Fig. 9. Covered normal fault in Sarmatian tuffitic sandstone (in site 15) indicating E–W extension of the D5 phase. Along the normal concave upward/antilistric fault a syn-sedimentary wedge was formed. Close to the fault the sub-horizontal layers are folded due to drag effect or indicate an earlier extensional monocline above an upward propagating normal fault.

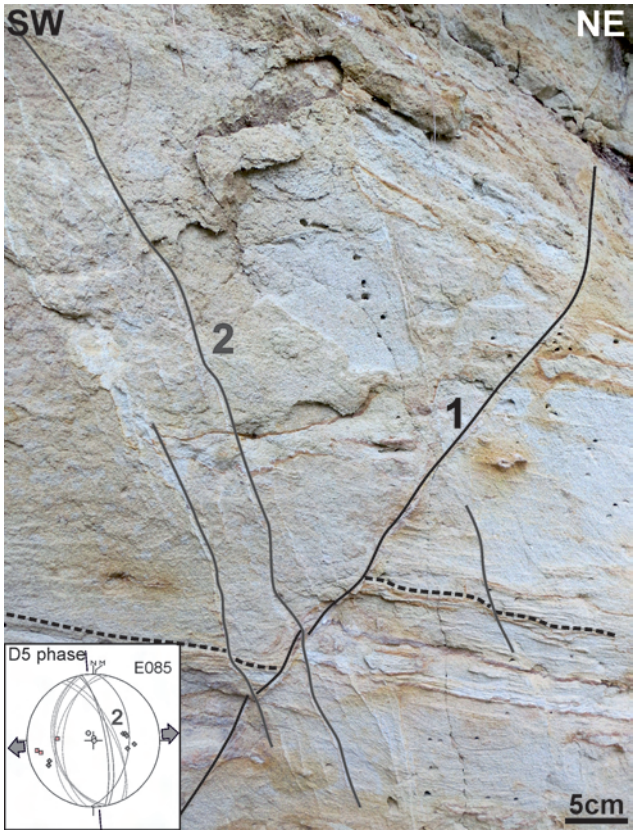

Fig. 10. Two sets of deformation band crosscut each other at site 16. The first **(1)** generation of bands with almost decimetre offset are crosscut by numerous younger bands **(2)** with smaller, cm scale offsets, all related to the D5 phase.

were detected indicating rejuvenation of the D5 phase fault during the D6 phase (Fig. 11).

In the Vatta-Maklár Trough the upper volcanoclastic units and Sarmatian sandstone are thickened in the hanging-wall block of the NE–SW trending faults and are pinching out north-westward, at the margins of the half graben (Petrik et al. 2014). These faults might have acted as oblique sinistral ones during the D5 phase. These faults crosscut the older Paleogene reverse faults making the subsurface structure more complicated (Figs. 6, 7). The observed syn-tectonic thickening represents the third major tilting event (Fig. 3).

Paleomagnetic data indicates no rotation for the upper volcanoclastic units (Márton & Pécskay 1998). The age of this deformation is well constrained as Middle Badenian-early Sarmatian.

D6 phase (late Sarmatian)

This phase is characterized by extension ranging from WNW–ESE to NW–SE direction (Fig. 4, sites 1, 5, 10, 12, 14, 15). NNE–SSW trending normal faults of phase D5 were often reactivated as oblique normal faults during the D6 phase due to the continuous CW change of extensional direction (sites 12, 15 in Fig. 4 and Fig. 11). This deformation was observed in Sarmatian sandstone and in the rocks of the upper volcanoclastic level in the DDB and FG areas. Several metres of normal displacement in Sarmatian sandstone was detected in the western margin of the FG area. In the northwestern part of the DDB (Fig. 4, site 10) this deformation is well represented by conjugate NE–SW trending normal faults.

The FG is filled with Sarmatian and upper volcanoclastic units but further to the west they also outcrop in the hanging-wall blocks of NNE–SSW trending normal faults (Fig. 7). On NW–SE trending seismic profiles the thickening of Sarmatian units are also presumed based on borehole data (Verps-2, Verps-3, Esz-1) (Figs. 2, 6).

In the Southern Bükk foreland some NW–SE trending reverse faults and small scale associated folds also belong to this phase (Fig. 4, site 5). In site 14, N–S and ENE–WSW trending dextral and sinistral strike-slip faults were observed, respectively. These strike-slip or compressional features differ in style from normal faulting, but, due to the similarity in the horizontal stress axes, could be classified into the D6 phase.

The age of this deformation is late Sarmatian and predates the early Late Miocene major tilting event.

Post-rift deformation

D7 phase (early Late Miocene)

Pannonian sediments only outcrop in the southernmost part of the DDB but the outcrop conditions do not allow a detailed study (Fig. 2). In the southern Bükk foreland ENE–WSW oriented normal fault and deformation bands can be found in early Late Miocene sandstone and indicate NNW–SSE extension (Fig. 4, site 17). All the small-scale structures of the D7 phase show syn-tilt deformation with respect to the early Late Miocene tilting event proven by tilt test (Fig. 4, sites 1, 3, 6, 13, 17). On seismic profiles the Middle Miocene rocks are often truncated and onlapped by Late Miocene sediments indicating early Late Miocene tilting (Fig. 6) (Petrik et al. 2014). In the entire South Bükk foreland and Vatta-Maklár Trough the Pannonian sediments are syn-sedimentary, thickening southward along ENE–WSW trending normal faults (Petrik et al. 2014). Although the outcrop-scale faults show somewhat younger timing, we assume that the large-scale faulting seen on seismic lines are marked by NNE–SSW extension of the D7 phase.

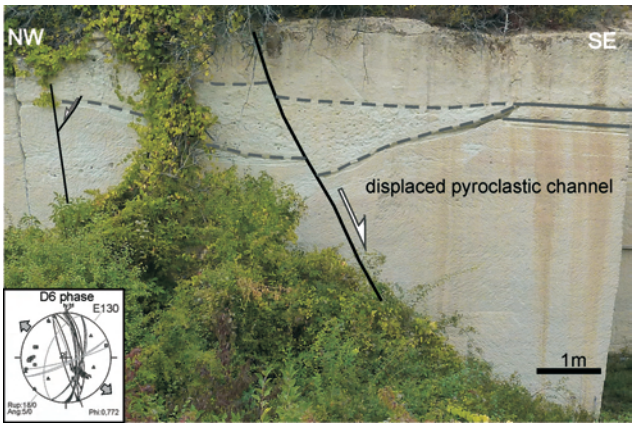

Fig. 11. N–S trending oblique normal fault of the D6 phase which displaced a channel filled with pyroclastic rocks (in site 12). The fault could be originated in phase D5 as dip-slip normal fault.

Discussion

Interpretation of the main structural phases and their implications for the evolution of the study area

Seven main structural phases were delineated in the study area from the Late Oligocene up to early Late Miocene (Figs. 4, 12). The combined usage of field observations, borehole data and seismic interpretation allowed us to determine new structural phases and to outline the Cenozoic structural evolution of the DDB in much more detail than in the previous studies (e.g., Tari 1988; Csontos 1999; Fodor et al. 1999, 2005). In addition, we connected the deformation phases of the Southern Bükk Foreland of Petrik et al. (2014) to those of the DDB sensu stricto (Fodor et al. 2005). The delineated stress fields were classified as pre-, syn-, and post-rift phases with respect to the evolution of the Pannonian Basin although this classification may need revision in the near future.

Pre-rift deformations

Two structural phases can be tied to pre-rift deformations (Figs. 4, 12).

The **D1 phase** is mainly characterized by NW–SE compression and perpendicular extension during the Eocene?–early Eggenburgian (Fig. 4). All the structures belonging to this phase indicate pre-tilt deformation with respect to the second major tilting (ca. 20–19 Ma).

The time of this deformation is well constrained by a syn-sedimentary dilational band of Late Oligocene age (Fig. 12)

(Petrik et al. 2014). The duration of the D1 phase can be extended into the early Eggenburgian because deformation bands in Eggenburgian site 7 (~21.4–20.9 Ma) also belong to this phase.

The syn-sedimentary thickening of Paleogene sediments in front of NW-vergent blind reverse faults postulated on seismic profiles was also attributed to our D1 phase. In the Vatta-Maklár Trough, several hundred metres of poorly dated terrestrial sediments below the lower volcanoclastic level were possibly deposited during the D1 phase (Fig. 6, Petrik et al. 2014). The certainly Oligocene rocks are strongly reduced and the poorly dated lower Miocene sediments are completely missing on earlier elevated highs underlain by NW-vergent blind reverse faults (Fig. 6) (Földvári 2013; Petrik et al. 2014). Erosion of Oligocene and sediments on elevated highs can be tied to the first denudation phase and associated tilting events (Figs. 3, 12).

The NNE–SSW oriented Darnó Line acted as a NW-vergent reverse fault which resulted in the formation of a syncline west of the Darnó Line (Fig. 1b) (Sztanó & Tari 1993; Fodor et al. 2005). In this syncline the Paleogene and Eggenburgian sediments are folded and thickened toward the reverse fault (Fig. 1b) (Fodor et al. 2005). In addition to NW-propagating reverse faults, some SE-vergent reverse faults were also detected on seismic profiles in the Vatta-Maklár Trough and were interpreted as small-scale backthrusts (Fig. 6, below borehole Verps-3, (Petrik et al. 2014).

We projected the seismic interpretation into the area of the Felsőtárkány graben (FG) in order to trace and correlate the major NE–SW trending faults further to the NE. We presume that one branch of the Paleogene basin could be found below the Felsőtárkány graben (FG). Our interpretation suggests that the precursor structure of the FG was bordered by a NE–SW trending fault on its eastern side which could have acted as a NW-vergent blind reverse fault during the Late Oligocene–earliest Miocene (Fig. 13a,b). Below the Middle Miocene sediments in the FG we presume wedge-shaped Paleogene rocks which pinched out northwestwardly on the next Mesozoic high (Fig. 7). No Paleogene sediments were encountered by boreholes on this high and this lack extends to the west, up to the Darnó Line. On the western side of the FG (on the Pirittyó Hill) a blind SE-vergent backthrust can

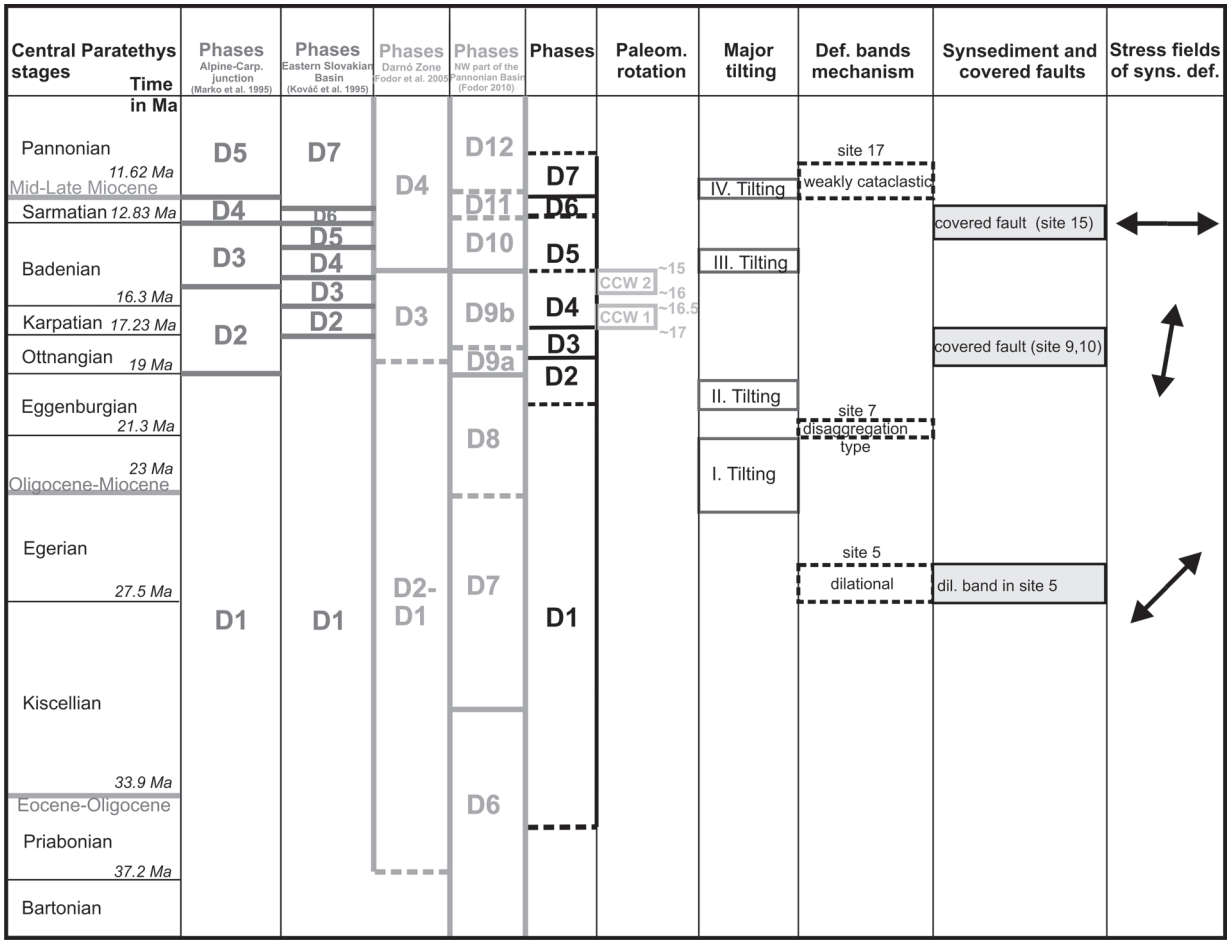

Fig. 12. Summary table about the possible time of deformation phases, CCW block rotations. Deformation bands and syn-sedimentary structures are also placed in time along with their stress fields. References for standard stages/Central Paratethys stages and their absolute ages see Fig. 3. Structural phases of the Darnó Zone (Fodor et al. 2005), the whole northern Pannonian unit (Fodor 2010), the Eastern Slovakian Basin (Kováč et al. 1995) and the Alpine-Carpathian Junction Zone (Marko et al. 1995) were also displayed to make comparisons with our new stress field data.

also be attributed to the erosion of Paleogene sediments (Figs. 7, 13a,b). The same architecture was found on NW–SE oriented seismic profiles 15 km to the southwest (Fig. 6). The seismic profiles indicate that the Esz-1 borehole drilled through the Lower Miocene rocks directly above the Mesozoic rocks (Fig. 6).

NW propagating Late Oligocene reverse faults were also identified ca. 75 km to the SW of the study area (Palotai & Csontos 2010). Tari et al. (1993) presumed that the Paleogene Basin was developed as a retroarc flexural basin by southward propagating backthrust along the northern margin of the NHSSPB (North Hungarian-South Slovakian Paleogene Basin).

In summary we assume that the studied part of the NHSSPB was characterized by NW-vergent folds and underlying blind reverse faults which resulted in the formation of synformal sub-basins with syn-tectonic fill (Fig. 13a,b). One of the major faults could be the Darnó Fault. Small-scale SE-vergent backthrusts could also evolve. On the other hand, the coeval existence of extensional and compressional structures of the D1 phase can be interpreted as noticeable elongation along the axis of the compressional folds (Fig. 13b). We agree with Tari et al. (1993) that, in general, the NHSSPB represents a flexural basin, but its postulated boundary is out of our study area, while our dataset characterize its internal structure.

The D2 phase is represented by W–E compression and perpendicular extension during the middle Eggenburgian–early Ottnangian (Fig. 4). The deviation in σ_1 can reach 30–40° with respect to the D1 phase in the counterclockwise sense. The D2 phase includes mainly strike-slip faults. The structures belonging to this phase indicate post-tilt and partially syntilt deformation with respect to the second major tilting event which occurred ca. 20–19 Ma (Figs. 3, 12). In the Eggenburgian conglomerate near the Darnó Hill (Fig. 4, site 7) this type of deformation is represented by conjugate cataclastic deformation bands. In the lower volcanoclastic units this D2 phase is already missing thus the age of this stress field is middle Eggenburgian–early Ottnangian.

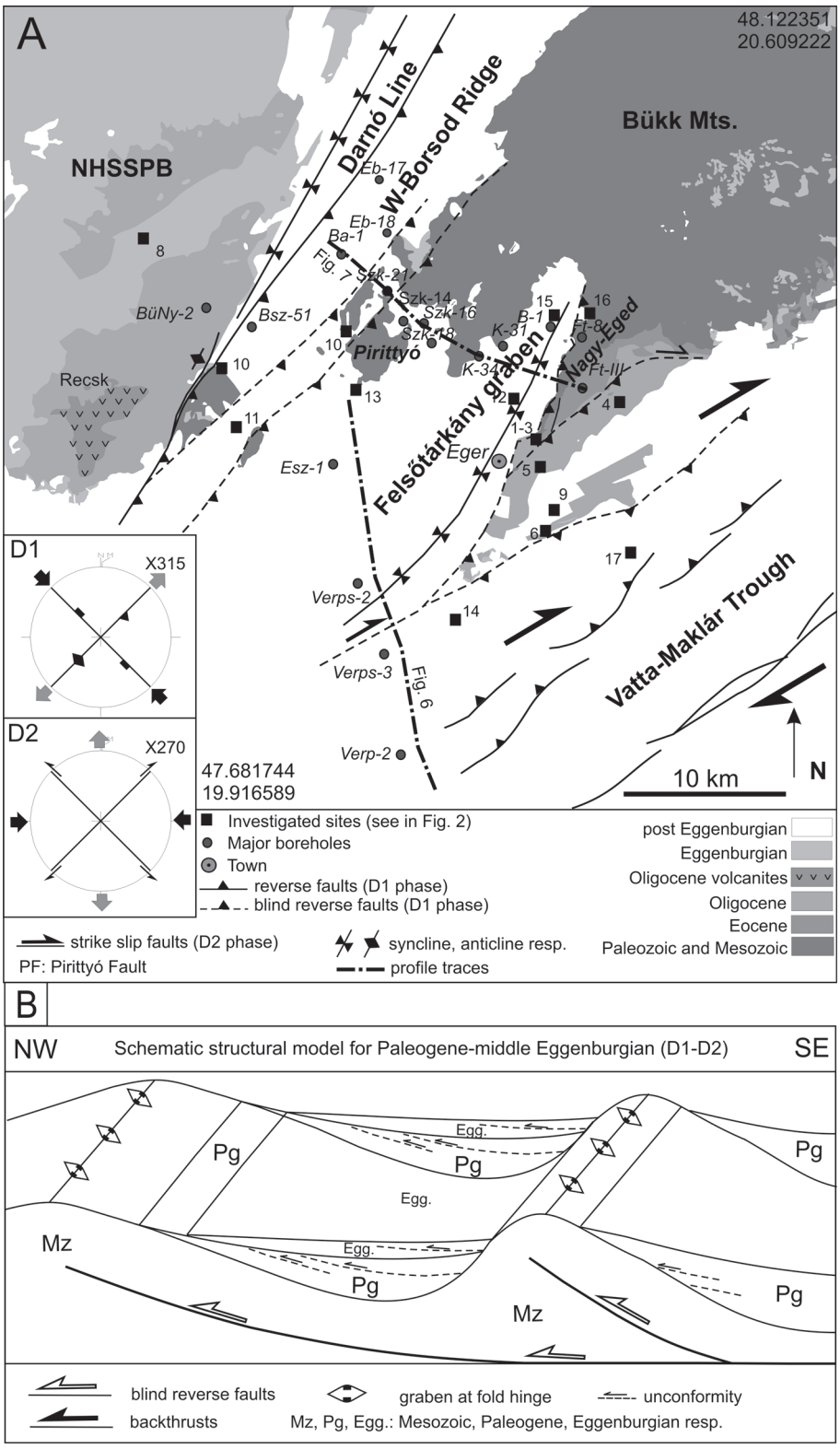

Fig. 13. A — Schematic structural pattern of the study area for the time of the D1-D2 phases (pre-rift deformation). Note the NE–SW trending blind reverse faults of the D1 phase. **B** — Schematic structural model for the time of the D1-D2 phases. See details in the text.

It is difficult to identify map-scale faults of this phase, but we assume that some of the reverse faults, particularly the steeper ones, could be reactivated as dextral faults (Fig. 13a). On the other hand, the D2 stress field could characterize the Mid-Hungarian Shear Zone, and the extrusion/escape tectonics of the Alcapa block (Csontos & Nagymarosy 1998).

A new definition of phases D1 and D2 with respect to earlier works

We suggest a new age limit for the D1 and D2 phases. Earlier works either did not separate them or gave different temporal boundaries. Csontos (1999) defined NE–SW and NW–SE compression for the Eocene–Early Oligocene and Late Oligocene times, respectively. The latter could be correlated with our D1 phase. Fodor et al. (1999, 2005) could not separate clearly the Paleogene-Early Miocene deformations. On the other hand, Fodor (2008, 2010) suggested three Paleogene–Early Miocene phases, D6, D7, and D8 between 48–19 Ma (Fig. 12). All these phases, together, were regarded as one of the most important deformations in Northern Hungary. However, the age limits are different.

D6 indicates mainly transpressional deformation with WNW–ESE and NW–SE shortening during the Middle Eocene–early Kiscellian (Fodor 2008); the beginning of our D1 phase could partially overlap with the end of the D6 phase (Fig. 12). D7 was characterized by NW–SE compression and perpendicular extension in the late Kiscellian–early Egerian (Fodor 2008); but our D1 phase was longer than in earlier works. The D8 phase indicates E–W compression and perpendicular extension with strike slip deformation prior to Ottnangian (Fodor 2010); however, our D2 phase started later than in earlier works (Fodor et al. 1999; Fodor 2010). The strike-slip character and the stress axes of his D2 (earlier D8 phase) clearly separates it from the earlier D1 phase. On the other hand, this D2 phase lasted somewhat longer than in previous works, and includes the early Ottnangian (Fig. 12) because it includes partially post-tilt deformation with respect to a second major tilting (ca. 20–19 Ma). If we accept that this phase is characterized by the extrusion tectonics, it would have a smaller time span than in previous works (Csontos & Nagymarosy 1998; Fodor et al. 1999).

Looking to a wider regional comparison, we also see observations of similar stress fields to our D1 and D2 phases. As we show briefly, and with two examples on Fig. 12, these suggested phases have different time spans than our phases.

In the Alpine-Carpathian Transition Zone (ACTZ) the WNW–ESE to NW–SE compression was dominant during the Oligocene-Eggenburgian time (D1 phase of Marko et al. 1995 in Fig. 12) which was similar to our D1, and partly to our D2 phase. In the northern margin of the Danube Basin, similar NW–SE compression was delineated for the Eggenburgian (Marko 2012). The syn-sedimentary activity of the Central Slovakian Fault System (CSFS) in the Central Western Carpathians was dated to the Late Eocene when NW–SE compression created a sinistral transtensional fault zone (Kováč & Hók 1993).

In the Eastern Slovakian Basin (ESB) the NNE–SSW to NE–SW compression was dominant during the Paleogene-Ottnangian (D1 phase of Kováč et al. 1995 in Fig. 12) resulting in the break-up of the Central Carpathian Paleogene Basin and folding of the Pieniny Klippen Belt (Kováč et al. 1995). This phase was terminated by an uplift and denudation event in the Ottnangian (Kováč et al. 1995).

Most of the delineated stress fields indicate WNW–ESE to NW–SE compression or transpression which are similar to our D1 phase but the time span is different ranging from Late Eocene to early Ottnangian. Marko et al. (1995) determined the upper limit of the D1 phase in the late Eggenburgian–early Ottnangian as opposed to our D1 phase which terminated in the early Eggenburgian. Kováč et al. (1995) identified the opposite compressional direction in the ESB which lasted until the late Ottnangian (D1 phase in Fig. 12). This difference in compressional direction is a spatial one, and might be explained by the curved geometry of the Carpathian orogen (Jiříček 1981).

Syn-rift deformations

The D3 phase is characterized by NNE–SSW extension during the late Ottnangian–early Karpatian (Fig. 4). The position of stress axes during phase D3 is similar to the situation during D2, but D3 clearly involves extensional deformation which is a striking difference from the pre-rift deformations. Fodor (2010) separated the early syn-rift episodes into a N–S and a NE–SW extensional one. Our D3 phase would correspond to his regional N-S extensional stress field. According to Fodor (2010) this stress field started during the early Ottnangian but must have finished before the first CCW block rotation (~18.5–17.5 Ma, Márton & Pécskay 1998). Our observations can refine the time span of this deformation. The D3 phase was syn-sedimentary during the late Ottnangian to earliest Karpatian (Figs. 8a,b, 12). Accepting this refined time span of the D3 phase, the time of the first CCW rotation seems to be younger (~17.0–16.5 Ma) than previously thought (Fig. 12). On the other hand, the end of the escape tectonics would also be younger by 1 Myr.

The D3 phase resulted in the formation of some WNW–ESE trending map-scale normal faults in the DDB area (Figs. 2, 14a,b). The Darnó Line was claimed to act as a sinistral strike-slip fault during Ottnangian–Middle Badenian but some shortening and folding along restraining bends were also presumed (Fodor et al. 2005).

In our interpretation, the NNE–WSW trending major faults might have been inactive at this time and the WNW–ESE trending normal faults took up the deformation (Fig. 14a,b). In the hanging-wall blocks of these normal faults small scale thickening of Ottnangian–Karpatian sediments could be observed in the DDB area (Figs. 7, 14a,b).

The western side of the Western Carpathians suffered transpression with N–S maximal compression during the Ottnangian–Early Badenian (D2 phase of Marko et al. 1995 in Fig. 12). In the northern margin of the Danube Basin NW–SE to N–S compression was identified for the Ottnangian–early Karpatian time (Marko 2012).

During the Karpatian the stress field changed from transpression to transtension in the ESB (Kováč et al. 1995).

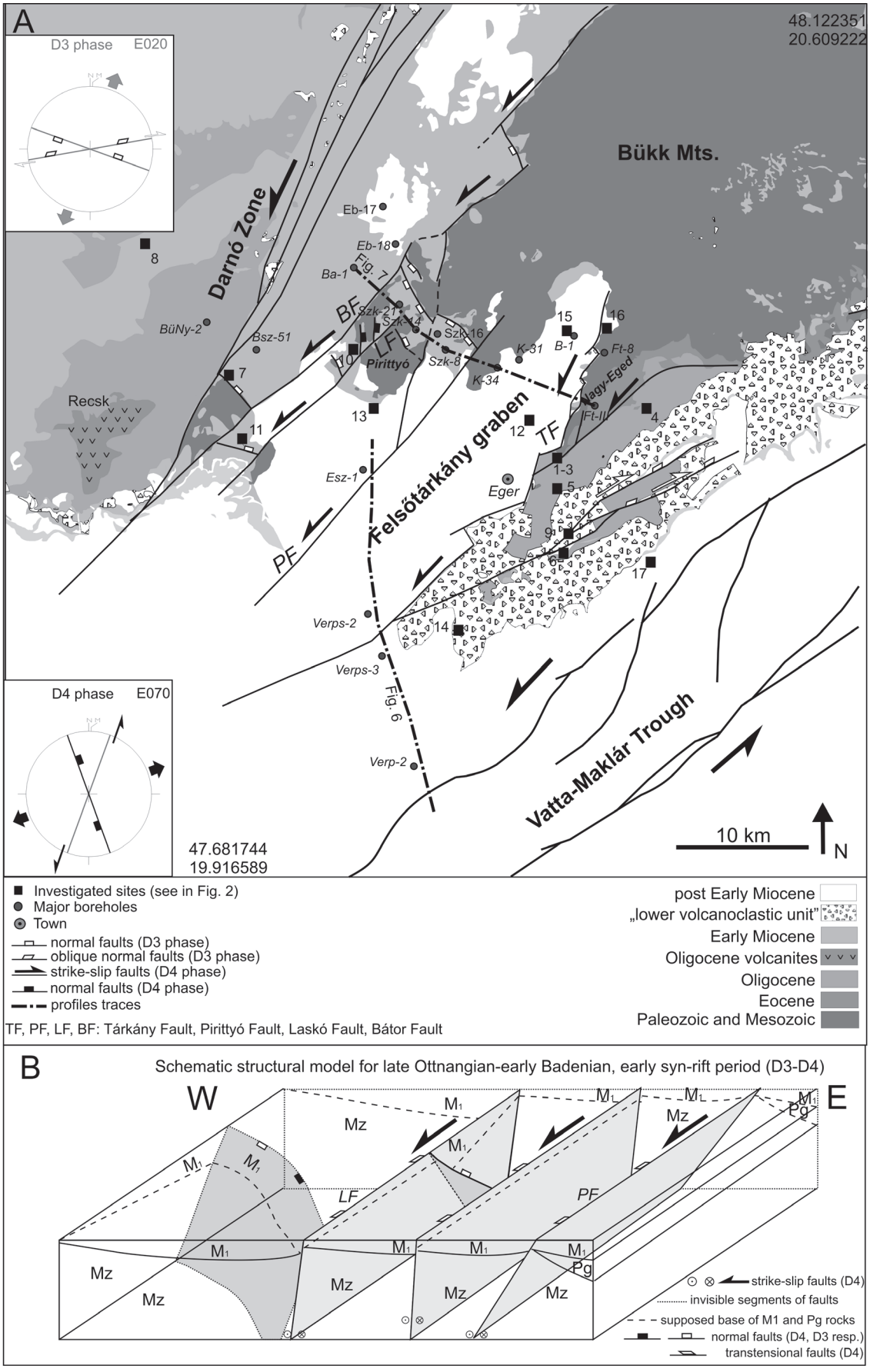
A
D3 phase E020
D4 phase E070
48.122351
20.609222
47.681744
19.916589
Bükk Mts.
Darnó Zone
Recsk
Felsőtárkány graben
Vatta-Maklár Trough
Pirittyó
Eger
Eb-17
Eb-18
Ba-1
Fig. 7
BüNy-2
Bsz-51
Szk-21
Szk-14
Szk-16
Szk-8
K-31
K-34
B-1
Ft-8
Nagy-Eged
Ft-II
Esz-1
Verps-2
Verps-3
Verp-2
Fig. 6
TF
PF
LF
BF
10 km
N
Investigated sites (see in Fig. 2)
Major boreholes
Town
normal faults (D3 phase)
oblique normal faults (D3 phase)
strike-slip faults (D4 phase)
normal faults (D4 phase)
profiles traces
TF, PF, LF, BF: Tárkány Fault, Pirittyó Fault, Laskó Fault, Bátor Fault
post Early Miocene
„lower volcanoclastic unit"
Early Miocene
Oligocene volcanites
Oligocene
Eocene
Paleozoic and Mesozoic
B
Schematic structural model for late Ottnangian-early Badenian, early syn-rift period (D3-D4)
W
E
Mz
M1
Pg
LF
PF
strike-slip faults (D4)
invisible segments of faults
supposed base of M1 and Pg rocks
normal faults (D4, D3 resp.)
transtensional faults (D4)

The ESB was opened as a pull-apart basin by N–S compression (D2 phase of Kováč et al. 1995 in Fig. 12). Our D3 phase covers a different time span and indicates N–S synsedimentary extension. This difference in stress fields might be explained by the paleo-geographical positions of the two regions. In our study area the D3 phase indicates the initial syn-rift deformation of the Pannonian Basin (Fodor 2010), while in the Western Carpathians the last phase of collision might have influenced the stress field suppressing the extension.

The D4 phase is represented by NE–SW and ENE–WSW extension during late Karpatian–Early Badenian (Fig. 4). This deformation was already present in the middle volcanoclastic units in the south Bükk foreland and in Early Badenian rocks in the DDB area. A clear relative chronology can be seen between D3 and D4 because the E–W trending normal faults of D3 tend to be reactivated as dextral-oblique faults during the D4 phase (Fig. 4, sites 6, 8). The extensional direction moved continuously in a CW direction from the Ottnangian onward as already stated by Fodor et al. (1999). The stress field evolution can be correlated with paleomagnetic data (Márton & Fodor 1995). The change in the principal stress axes between the D3 and D4 phases is similar in magnitude to the vertical-axis rotation, and opposite in sense. Thus, the change in stress field is apparent and connected to rotation.

Based on paleomagnetic measurements, the middle volcanoclastic units indicate 25–30° CCW rotation and suffered only the second CCW block rotation which occurred ~15–14 Ma (Márton & Fodor 1995). This means that the D4 phase post-dates the first CCW rotation and predates the second one. Our observations would suggest a late Karpatian–Early Badenian timing (Fig. 12). This phase can be regarded as the classical syn-rift deformation in the Pannonian basin which relates to the roll back mechanism triggered by the subducted slab below the Outer Carpathians (Royden & Horváth 1988). Our D4 corresponds to the D9b phase of Fodor (2010) and D3 of Fodor et al. (2005). This phase was responsible for the birth of many pull-apart sub-basins and half-grabens along NNE–SSW trending sinistral strike-slip and NW–SE trending normal faults, respectively, (Royden & Horváth 1988; Fodor et al. 1999).

This time the NNE–SSW trending major faults in the DDB area might have acted as sinistral faults (Fig. 4, site 11; Fig. 14a,b). NW–SE trending normal faults could evolve between the major NNE-SSW trending sinistral strike-slip faults (Fig. 14a,b).

In the ACTZ, the D2 phase of N–S compression continued until the Early Badenian. In the ESB, NE–SW extension was characteristic of the Early and Middle Badenian (D3+D4 phases of Kováč et al. 1995 in Fig. 12, which were similar to our D4 phase). These phases were responsible for cessation of strike-slip tectonics and the evolution of back-arc basins (Kováč et al. 1995). Although the time span is shorter in our area, the similarity of these phases can be explained by the influence of the roll-back mechanism of the subducted slab along the Outer Carpathians.

The D5 phase is represented by E–W to WNW–ESE extension/transtension during the Middle Badenian–early Sarmatian (Fig. 4). N–S oriented conjugate normal faults were dominant in the sites of the FG and DDB (Fig. 4, sites 12, 13, 15, 16). Covered normal faults in Sarmatian sandstone of the FG indicate E–W extension (Figs. 9, 12). The relative chronology between D4 and D5 is marked by reactivated earlier NW–SE trending normal faults as oblique dextral ones during the D5 phase. The syn-sedimentary thickening and tilting of upper volcanoclastic units and Sarmatian sediments along NNE–SSW trending faults were also interpreted on seismic profiles and geological cross sections (Figs. 6, 7). In our view, the FG is bordered on the east by a major NNE–SSW segmented transtensional fault (TF, Tárkány Fault) with sinistral-normal components based on the extensional direction of D5. The TF was responsible for the beginning of the subsidence of the FG in the late Mid Miocene (Fig. 15a,b). This transtensional fault can be correlated with NNE–SSW trending faults identified on seismic profiles (Fig. 6). The TF is often segmented along-strike and connected by small E–W oriented faults (Figs. 2, 15a,b). Small blocks of Paleogene to Early Miocene surrounded by late Mid-Miocene rocks on the eastern side of the FG are interpreted as fault lenses (Fig. 15a). We assume that the other NNE–SSW oriented faults in the DDB area (such as Felnémet Fault FF, Bátor Fault BF, Pirittyó Fault PF) also acted as sinistral-normal faults (transtensional faults) during the D5 phase (Figs. 2, 15a,b). In the south-western part of the DDB, the Mid-Miocene sediments are preserved in the hanging-wall blocks of NNE–SSW trending faults (FF, LF, PF) (Figs. 2, 15a,b).

In the Vatta-Maklár Trough the thickening of upper volcanoclastic and Sarmatian sediments along NE–SW oriented transtensional faults also started during the D5 phase (Petrik et al. 2014). According to Tari (1988) this was the time for the main subsidence of the Vatta-Maklár Trough. Fodor et al. (2005) also delineated this WNW–ESE extension for the Late Badenian onward. Csontos (1999) and Tari (1988) defined N–S compression and perpendicular extension with dominant strike-slip deformation for the Mid-Miocene period.

According to paleomagnetic measurements, the upper volcanoclastic units were not involved in the second CCW block rotation which took place ~15–14 Ma (Márton & Pécskay 1998). To take into consideration the syn-sedimentary late Mid-Miocene deformation of the D5 phase and the paleomagnetic data, the age of this phase is well-constrained and followed the second CCW blockrotation and could have lasted from the Late Badenian to early Sarmatian. However, the new zircon U-Pb age results of the upper pyroclastic units (15–14.0 Ma, Lukács et al. 2015) suggest that the age of the second CCW rotation could be somewhat older (between

Fig. 14. A — Schematic structural pattern of the study area for the D3-D4 phases. Note NNE–SSW trending sinistral faults of the D4 phase which are connected to WNW–ESE and NW–SE trending normal faults. **B** — Schematic structural model for the D3-D4 phases (early syn-rift). See details in the text.

~16–15 Ma). This means that the D5 phase could have started sometime in the Middle Badenian, earlier than previously thought (Fig. 12).

In the ACTZ, the transpression changed to transtension with WNW–ESE extension during the Middle Badenian. This resulted in the opening of pull-apart basins along ENE–WSW oriented sinistral faults (D3 phase of Marko et al. 1995 in Fig. 12). In the northern Danube Basin NE–SW compression and perpendicular extension was identified for the Badenian which is similar to our D6 of Sarmatian age (Marko 2012). In the Middle Miocene a change in maximum compression can be observed from NW–SE to NE–SW in the CSFS area which acted even in the Late Miocene (Kováč & Hók 1993). This compression is similar to our D5-D6 phase but its time span is wider than our D5, D6 phases.

In the ESB, the Late Badenian is represented by NE–SW extension which resulted in transtensional deformation with NW–SE trending normal faults at its eastern margin and NNE–SSW trending dextral faults at its western margin (D5 phase of Kováč et al. 1995 in Fig. 12). This was the time for the main subsidence due to mantle upwelling (Kováč et al. 1995).

The D3 phase of Marko et al. (1995) indicates similar extension and a similar time span as our D5 phase. The D5 phase of Kováč et al. (1995) in the ESB indicates almost perpendicular extension and shorter time span than our D5 phase (Fig. 12). This difference in stress direction might be explained by the inhomogeneity of the stress fields in the Late Badenian–Sarmatian due to the changing (curved) geometry of the Outer Carpathian nappe front (Fodor & Csontos 1998).

The **D6 phase** is characterized by NW–SE extension during the late Sarmatian (Fig. 4). The deviation of minimal stress axis in a CW direction is continuous from Early Miocene onward. This phase clearly post-dates the D5 phase as is proven by oblique normal reactivation of N–S oriented normal faults of the D5 phase (Fig. 4, sites 12, 15). The youngest rocks involved in

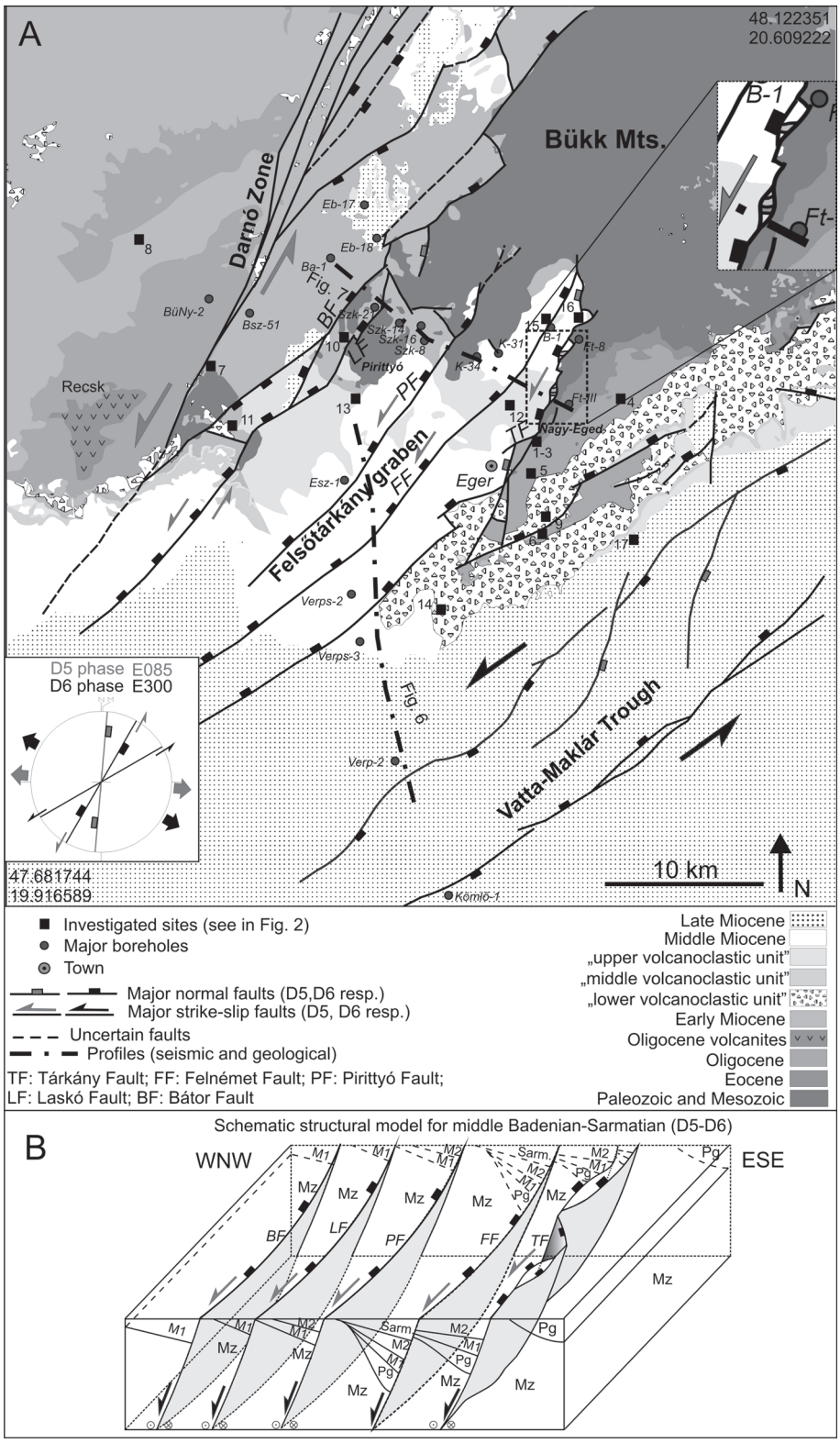

Fig. 15. A — Schematic structural pattern of the study area for the D5-D6 phases. Note the dominance of NNE–SSW trending transtensional (D5 phase) and normal faults (D6 phase). The inset in the north-eastern corner indicates the small fault lenses on the eastern side of the FG. **B** — Schematic structural model for the D5-D6 phases (late syn-rift). See details in the text.

this deformation are upper volcanoclastic units and Sarmatian sandstone. All structures belonging to this phase still indicate pre-tilt deformation with respect to early Late Miocene tilting (Fig. 12).

The NE–SW trending faults became pure extensional normal faults and induced further thickening of Sarmatian sediments in their hanging-wall blocks in the FG and in many small sub-basins up to the DDB (Fig. 15a,b). In our view, the Felsőtárkány graben (FG) became a half-graben which subsided continuously along the NE–SW trending TF during the Sarmatian although the kinematics might have slightly changed from D5 to D6. This is proven by south-eastward tilting and thickening of Sarmatian sediments in the FG (Fig. 7). Similar fault kinematics and subsidence were proven in the Vatta-Maklár Trough at that time (Petrik et al. 2014).

In the western part of the DDB (Eb-17 and Eb-18 boreholes in Fig. 2), the average values of vitrinite reflectance data deriving from Ottnangian sediments are ~0.27–0.29 % (Iharosné Laczó 1982). Similar vitrinite values were measured at ~100 m depth from early Late Miocene sediments in the southern Bükk foreland where they were interpreted as indications of at least 600–700 m burial depth during the Late Miocene (Petrik et al. 2014). This means that older rocks now on the surface used to be covered by a few hundred meters of sediments that have been eroded. This could be the Sarmatian and Late Miocene suites. According to fission track data, at least ~1 km of sediments must have eroded from the Bükk Mts. since the Pliocene/Quaternary (Dunkl et al. 1994). The sporadic occurrences of Sarmatian and early Late Miocene sediments west of the FG can be explained by Pliocene/Quaternary uplifting of the Bükk Mts. (Dunkl et al. 1994).

In the ACTZ, the NW–SE extension associated with strike-slip deformation was dominant during the Sarmatian time which is similar to our D6 phase (D4 phase of Marko et al. 1995 in Fig. 12). In the northern Danube Basin the ENE–WSW compression was defined for the Sarmatian and early Pannonian. This compressional direction is similar to that indicated by the few compressional data from our D6 phase. This shortening may represent a short-term Sarmatian inversion as was suggested in other parts of the Pannonian Basin (Horváth 1995; Fodor et al. 1999). In the CSFS area the NW–SE extension resulted in NE–SW trending normal faults during the Late Badenian–Sarmatian time which is similar to our D6 phase.

In the ESB, the N–S extension was dominant in late Sarmatian–Pannonian (D7 phase of Kováč et al. 1995 in Fig. 12). This N–S extension is more similar to our D7 phase which was active in early Pannonian (Fig. 12).

Post-rift deformation

The D7 phase is represented by NNW–SSE extension during the early Late Miocene (Fig. 4). The extensional direction tends to rotate further into the CW direction. In the study area Pannonian sediments are scarce on the surface but in the southern Bükk foreland the E–W oriented conjugate normal faults and deformation bands belong to this phase and clearly indicate post-tilt deformation with respect to earliest Late Miocene tilting (Fig. 12). Csontos (1999) supposed N–S compression for the early Late Miocene based on reverse faults and folding of late Pannonian sediments in the South Bükk foreland. This compression might indicate a short period of intra-Pannonian inversion. Tari (1988) defined an ENE–WSW trending transtensional deformation along the Vatta-Maklár Trough for the late Pannonian which can be fitted into our D7 phase.

Early Late Miocene sediments are syn-sedimentary and thickened toward the NE–SW trending transtensional fault in the Vatta-Maklár Trough between 11.6–8.92 Ma (Petrik et al. 2014). We suppose that early Late Miocene rocks used to cover the DDB area but due to the Pliocene/Quaternary uplift of the Bükk Mts. they were tilted 2–3° to the south and eroded in the northern part. On NW–SE oriented seismic profiles, the Pannonian sediments are tilted and truncated to the north close to the Bükk Mts. (Petrik et al. 2014).

In ACTZ, the NW–SE extension was responsible for creating host-graben structures along NE–SE trending normal faults (D5 phase of Marko et al. 1995 in Fig. 12). Many grabens and half-grabens subsided along NE–SW trending normal faults in the Pannonian (Kováč et al. 2011a). In the northern Danube Basin, E–W extension was delineated for the Pannonian time (Marko 2012) which indicates almost perpendicular extension in comparison with our D7 phase and also seems to be different from other Western Carpathian stress fields. It could be a local phase. In the Turiec Basin in the interior of the Western Carpathians, NW–SE extension and perpendicular compression was identified. This induced syn-rift deformation of the basin (Kováč et al. 2011b).

In the ESB, the N–S extension was dominant in the late Sarmatian-Pannonian which is similar to our D7 phase (D7 phase of Kováč et al. 1995 in Fig. 12). The majority of stress fields indicate NW–SE to NNW–SSE extension for the Pannonian time which indicates that the northern part of the Pannonian Basin was under the same stress regime.

Conclusions

The combined usage of detailed structural field observations, seismic interpretation and geological cross sections allowed us to delineate 7 deformation phases in the study area for the Cenozoic period.

The D1 and D2 phases are pre-rift deformations in the evolutionary history of the Pannonian Basin. The **D1** phase is pre-tilt with respect to the earliest Miocene tilting event. D1 indicates NW–SE compression and perpendicular extension for the Paleogene–early Eggenburgian time based on an early type of deformation bands and syn-sedimentary thickening of Paleogene suites in front of NE–SW trending north-westward propagating blind reverse faults. This phase was recognized earlier but we were able to specify the upper age limit of this phase and put it into the early Eggenburgian based on deformation in Eggenburgian conglomerate. The coeval existence of extension and compression can be explained by noticeable elongation along the axis of the compressional folds.

D2 is a middle Eggenburgian–early Ottnangian post-tilt phase which indicates strike-slip deformation. The erosion of Paleogene sediments above elevated highs could partly be associated with this phase. West of the Darnó Line, the folding of Eggenburgian and reversely displaced pre-Ottnangian sediments was also associated with ongoing shortening deformation with strike slip components (Fodor 2010).

The D3 and D4 stress fields belong to early syn-rift phases and indicate pre-tilt deformation with respect to early Late Miocene tilting.

Phase **D3** shows NNE–SSW extension and it is a well-constrained stress field based on syn-sedimentary deformation of Ottnangian–early Karpatian sediments and covered normal faults in the lower volcanoclastic unit. This phase predates the first CCW rotation which has been specified and placed between ~17.0–16.5 Ma in the Karpatian. Fodor (2010) stated that this stress field must predate the escape of the ALCAPA unit. Consequently, the extrusion tectonics may terminate somewhat later by ca. 1 Myr. In our view, the NNE–SSW trending faults of the DDB were inactive at this time. WNW–ESE trending normal faults could have been developed inducing the small-scale thickness variations of Early Miocene sediments.

The **D4** phase can be regarded as a classical syn-rift phase indicating NE–SW extension for the late Karpatian–Early Badenian. This phase postdates the first CCW rotation and it was responsible for creating NW–SE trending normal faults which connect the major NNE–SSW trending sinistral faults.

The D5 and D6 phases are late syn-rift deformations. Phase **D5** shows E–W extension during the Middle Badenian–early Sarmatian constrained by syn-sedimentary deformation in early Sarmatian tuffitic sandstone. The syn-sedimentary thickening of upper volcanoclastic units and Sarmatian sediments along NNE–SSW trending sinistral-normal faults was also identified. The D5 phase was responsible for the beginning of the development of the Felsőtárkány graben (FG) along a NNE–SSW trending transtensional fault. We suggest that the majority of NNE–SSW trending faults (PF, LF, BF, TF, FF) acted as normal-sinistral faults during the D5 phase. This phase postdates the second CCW rotation. We were able to specify the lower time limit of this deformation which was previously thought to have started in the Late Badenian (Fodor et al. 2005).

D6 clearly postdates the D5 phase and indicates pure NW–SE extension in the Sarmatian before early Late Miocene tilting. This phase promoted ongoing subsidence along NNE–SSW trending faults in the DDB area and it was also responsible for creating half grabens (e.g. Felsőtárkány graben).

The D7 phase is a post-rift deformation partly coeval with the early Late Miocene tilting. This indicates NNE–SSW extension during 11.6–8.92 Ma. The sporadic occurrence of Late Miocene sediments can be tied to Pliocene/Quaternary uplift and erosion of the Bükk Mts. as fission track and vitrinite reflectance data indicate.

Acknowledgements: Our investigation was supported by the Hungarian National Research Fund (OTKA No. 81530). We are grateful to the Hungarian Horizon Ltd. and MOL Ltd. for providing us with seismic data. We thank Elsevier for allowing us to reuse one of our earlier published figures (Fig. 6, Petrik et al. 2014). Réka Lukács' work was supported by the Hungarian National Research Fund (OTKA-PD112584) and by the Bolyai János Research Fellowship.

References

Anderson E.M. 1951: The dynamics of faulting and dyke formation with application to Britain. 2nd edition. *Oliver & Boyd*, Edinborough, 1–206.

Angelier J. 1984: Tectonic analysis of fault slip data sets. *J. Geophys. Res.* 89, B7, 5835–5848.

Angelier J. 1990: Inversion of field data in fault tectonics to obtain the regional stress. III. A new rapid direct inversion method by analytical means. *Geophys. J. Internat.* 103, 363–373.

Angelier J. & Manoussis S. 1980: Classification automatique et distinction des phases superposée en tectonique de failles. *C.R. Acad. Sci. Paris* 290, série D, 651–654 (in French).

Ádám L. 2006: Sequence stratigraphy, age and paleogeography of the Miocene coals along Sajó river. *PhD Thesis, Eötvös University,* 1–100 (in Hungarian).

Báldi T. 1986: Mid-Tertiary stratigraphy and paleogeographic evolution of Hungary. *Akadémia Press*, Budapest, 1–201.

Báldi T. & Báldi-Beke M. 1985: The evolution of the Hungarian Paleogene Basins. *Acta Geol. Hung.* 28*,* 1–2, 5–28.

Báldi T. & Sztanó O. 2000: Gravity mass movements and paleobathymetric changes in the marine Oligocene deposits of the Bükk Mts. *Földt. Közl.* 130, 3, 451–496 (in Hungarian).

Bergerat F., Geyssant J. & Lepvrier C. 1984: Neotectonic outline of the Intra-Carpathian basins in Hungary. *Acta Geol. Hung.* 27, 237–251.

Csontos L. 1999: Structural outline of the Bükk Mts. (N Hungary). *Földt. Közl.* 129, 4, 611–651 (in Hungarian).

Csontos L. & Nagymarosy A. 1998: The Mid-Hungarian line: a zone of repeated tectonic inversion. *Tectonophysics*, 297, 51–72.

Csontos L., Nagymarosy A., Horváth F. & Kováč M. 1992: Cenozoic evolution of the Intra-Carpathian area: a model. *Tectonophysics,* 208, 221–241.

Dunkl I., Árkai P., Balogh K., Csontos L. & Nagy G. 1994: Thermal modelling based on apatite fission track dating: the uplift history of the Bükk Mts. *Földt. Közl.* 124, 1, 1–24 (in Hungarian).

Fodor L. 2008: Structural geology. In: Budai T. & Fodor L. (Eds.): Geology of the Vértes Hills. *Geol. Inst. of Hungary*, 145–202, 282–300.

Fodor L. 2010: Mesozoic and Cenozoic stress fields and fault patterns in the northwestern part of the Pannonian Basin — methodology and structural analysis. *Doctoral Dissertation of the Hungarian Academy of Sciences*, 1–167 (in Hungarian).

Fodor L. & Csontos L. 1998: Structural geological research in Hungary: a review. *Földt. Közl.* 128,1, 123–143 (in Hungarian).

Fodor L., Csontos L., Bada G., Györfi I. & Benkovics L. 1999: Tertiary tectonic evolution of the Pannonian Basin system and neighbouring orogens: a new synthesis of paleostress data. In: Durand B., Jolivet L., Horváth F. & Séranne M. (Eds.): The Mediterranean Basins: Tertiary extension within Alpine Orogen. *Geol. Soc. London, Spec. Publ.* 156, 295–334.

Fodor L., Jelen B., Márton E., Skaberne D., Čar J. & Vrabec M. 1998: Miocene–Pliocene tectonic evolution of the Slovenian Periadriatic Line and surrounding area — implication for Alpine-Carpathian extrusion models. *Tectonics* 17, 690–709.

Fodor L., Radócz Gy., Sztanó O., Koroknai B., Csontos L. &

Harangi Sz. 2005: Post-conference excursion: tectonics, sedimentation and magmatism along the Darnó Zone. *GeoLines* 19, 142–162.

Fodor L.I., Sztanó O., Magyar I., Törő B., Uhrin A., Várkonyi A., Csillag G., Kövér Sz., Lantos Z. & Tőkés L. 2013: Late Miocene depositional units and syn-sedimentary deformation in the western Pannonian basin, Hungary. In: Schuster R. (Ed.): 11th Workshop on Alpine Geological Studies & 7th European Symposium on Fossil Algae. *Abstracts & Field Guides*, Schladming, 99, 33–34.

Földvári J. 2013: The revision of the boreholes in Mezőkeresztes hydrocarbon field. *MSc. thesis, Eötvös University,* 1–62 (in Hungarian).

Fossen H., Schultz R., Shipton Z. & Mair K. 2007: Deformation bands in sandstone — a review. *J. Geol. Soc. (London)* 164, 755–769.

Fusán O., Plančár J. & Ibrmajer J. 1987: Tectonic map of basement of Tertiary in Inner Western Carpathians. *Geological Institute of Dionýz Štúr*, Bratislava.

Harangi S., Mason P.R.D. & Lukács R. 2005: Correlation and petrogenesis of silicic pyroclastic rocks in the Northern Pannonian Basin, Eastern-Central Europe: In situ trace element data of glass shards and mineral chemical constraints. *J. Volcanol. Geotherm. Res.* 143, 4, 237–257.

Hartai É. 1983: Some new acidic pyroclastite occurences in the Bükk Mountains. *Földt. Közl.* 113, 303–312 (in Hungarian).

Hohenegger J., Ćorić S., Khatun M., Pervesler P., Rögl F., Rupp C., Selge A., Uchmann A. & Wagreich M. 2009: Cyclostratigraphic dating in the Lower Badenian (Middle Miocene) of the Vienna Basin (Austria): the Baden-Sooss core. *Int. J. Earth. Sci*. 98, 915–930.

Iharosné Laczó I. 1982: The geological evaluation of Hungarian vitrinite reflectance values. *Ann. Report Geol. Inst. Hungary from 1982*, 417–437 (in Hungarian).

Jaskó S. 1946: The Darnó Line. *Summary of proceedings of the Hungarian Geological Institute*, 7, 63–77 (in Hungarian).

Jiříček R. 1981: Contact between Miocene deposits and alpino-type basement of the East Slovakian Neogene Basin. In: Grecula P. (Ed.): Geological Structure and raw materials in the Border Zone of the East and West Carpathians. *GÚDŠ*, Bratislava, 39–46 (in Czech).

Kázmér M. & Kovács S. 1985: Permian–Paleogene paleogeography along the Eastern part of the Insubric-Periadriatic Lineament system: Evidence for continental escape of the Bakony-Drauzug Unit. *Acta Geol. Hung.* 28, 71–84.

Kessler J. & Hír J. 2012: The avifauna in North Hungary during the Miocene. Part I. *Földt. Közl.* 142, 1, 67–78 (in Hungarian).

Kováč M., Kováč P., Marko F., Karoli S. & Janočko J. 1995: The East Slovakian Basin — A complex back-arc basin. *Tectonophysics*, 252, 453–466.

Kováč M., Synak R., Fordinál K., Joniak P., Tóth Cs., Vojtko R., Nagy A., Baráth I., Maglay J & Minár J. 2011a: Late Miocene and Pliocene history of the Danube Basin: inferred from development of depositional systems and timing of sedimentary facies changes. *Geol. Carpathica* 62, 6, 519–534.

Kováč M., Hók J., Minár J., Vojtko R., Bielik M., Pipík R., Rakús M., Kráľ J., Šujan M & Králiková S. 2011b: Neogene and Quaternary development of the Turiec Basin and landscape in its catchment: a tentative mass balance model. *Geol. Carpathica* 62, 4, 361–379.

Kováč P. & Hók J. 1993: The Central Slovak fault system — The field evidence of a strike slip. *Geol. Carpathica* 44, 3, 155–159.

Less Gy. 2005: Palaeogene. In: Pelikán P. & Budai T. (Eds.): Geology of the Bükk Mountains. *Geol. Inst. of Hungary*, 204–211.

Less Gy., Frijia G., Filipescu S., Holcová K., Mandic O. & Sztanó O. 2015: New Sr-isotope stratigraphy (SIS) age-data from the Central Paratethys. *2nd International Congress on Stratigraphy, Abstracts*, 223.

Less Gy., Gulácsi Z., Kovács S., Pelikán P., Pentelényi L., Rezessy A. & Sásdi L. 2005: Geological map of the Bükk Mountains 1:50.000. *Geol. Inst. of Hungary*.

Lukács R., Harangi Sz., Ntaflos T. & Mason P.R.D. 2005: Silicate melt inclusions in the phenocrysts of the Szomolya Ignimbrite, Bükkalja Volcanic Field (Northern Hungary): Implications for magma chamber processes. *Chem. Geol.* 223, 1–3, 46–67.

Lukács R., Harangi Sz., Mason P.R.D. & Ntaflos T. 2009: Bimodal pumice populations in the 13.5 Ma Harsány ignimbrite, Bükkalja Volcanic Field, Northern Hungary: syn-eruptive mingling of distinct rhyolitic magma batches? *Central Eur. Geol.* 52, 1, 51–72.

Lukács R., Harangi Sz., Ntaflos T., Koller F. & Pécskay Z. 2007: The characteristics of the Upper Rhyolite Tuff Horizon in the Bükkalja Volcanic Field: The Harsány ignimbrite unit. [A Bükkalján megjelenő felső riolittufaszint vizsgálati eredményei: a harsányi ignimbrit egység]. *Földt. Közl.* 137, 4, 487–514 (in Hungarian).

Lukács R., Harangi Sz., Bachmann O., Guillong M., Soós I., Dunkl I. & Fodor L. 2014a: New zircon U-Pb geocronological data to constrain the duration of the Si-rich Miocene volcanism in the Pannonian Basin. In: Pál-Molnár E. & Harangi Sz. (Eds.): Petrological processes from the mantle to the surface. V. *Petrological and Geochemical Assembly of Hungary*, 60–63 (in Hungarian).

Lukács R., Guillong M., Harangi Sz., Bachmann O., Fodor L., Dunkl I. & Soós I. 2014b: New zircon U-Pb geochronological data for constraining the age of the Miocene ignimbrite flare-up episode in the Pannonian Basin. *Buletini Shkencave Gjeologjike*, Special Issue 2014, 1, 238.

Lukács R., Harangi S., Bachmann O., Guillong M., Danišík M., Buret Y., von Quadt A., Dunkl I., Fodor L., Sliwinski J., Soós I. & Szepesi J. 2015: Zircon geochronology and geochemistry to constrain the youngest eruption events and magma evolution of the Mid Miocene ignimbrite flare up in the Pannonian Basin, eastern central Europe. *Contr. Mineral Petrology* 170, 52. Doi 10.1007/s00410-015-1206-8

Magyar I., Geary D.H. & Müller P. 1999: Paleogeographic evolution of the Late Miocene Lake Pannon in Central Europe. *Palaeogeogr. Palaeoclimatol. Palaeoecol.* 147, 151–167.

Majzon L. 1961: The stratigraphic subdivision of northern Hungarian Oligocene based on studies of forams. *Földt. Közl.* 91, 2, 121–125.

Marko F. 2012: Cenozoic stress field and faulting at the northern margin of the Danube Basin (Western Carpathians, Slovakia). *Miner. Slovaca* 44, 213–230 (in Slovak).

Marko F., Plašienka D. & Fodor L. 1995: Meso–Cenozoic tectonic stress fields within the Alpine-Carpathian Transition Zone: a review. *Geol. Carpathica* 46, 1, 19–27.

Márton E. 1990: Paleomagnetic studies on the Miocene volcanic horizons at the southern margin of the Bükk Mts. *Ann. Report of the Eötvös Loránd Geophys. Inst. of Hungary for 1988-89*, 211–217, 307–309.

Márton E. & Fodor L. 1995: Combination of paleomagnetic and stress data — a case study from North Hungary. *Tectonophysics* 242, 99–114.

Márton E. & Márton P. 1996: Large scale rotations in North Hungary during the Neogene as indicated by paleomagnetic data. In: Morris A. & Tarling D. (Eds.): Paleomagnetism and tectonics of the Mediterranean Region. *Geol. Soc. London, Spec. Publ.* 105, 153–173.

Márton E. & Pécskay Z. 1998: Complex evaluation of paleomagnetic and K/Ar isotope data of the Miocene ignimbritic volcanics

in the Bükk Foreland, Hungary. *Acta Geol. Hung.* 41, 4, 467–476.

Nagymarosy A. 1990: Paleogeographical and paleotectonical outlines of some Intracarpathian Paleogene Basins. *Geol. Carpathica* 41, 3, 259–274.

Palotai M. & Csontos L. 2010: Strike-slip reactivation of a Paleogene to Miocene fold and thrust belt along the central part of the Mid-Hungarian Shear Zone. *Geol. Carpathica* 61, 6, 483–493.

Pelikán P. 2005: Miocene Formations of the western and northern forelands. In: Pelikán P. & Budai T. (Eds.): Geology of the Bükk Mountains. *Geol. Inst. of Hungary*, 215–230.

Pentelényi L. 2005: Miocene pyroclastic beds in the Bükkalja. In: Pelikán P. & Budai T. (Eds.): Geology of the Bükk Mountains. *Geol. Inst. of Hungary*, 212–215.

Petrik A., Beke B. & Fodor L. 2014: Combined analysis of faults and deformation bands reveals the Cenozoic structural evolution of the southern Bükk foreland (Hungary). *Tectonophysics* 633, 43–62.

Popov S.V., Akhmetev M.A., Zaporozhets N.I., Voronina A.A. & Stolyarov A.S. 1993: Evolution of the Eastern Paratethys in the Late Eocene–Early Miocene. *Stratigr. Geol. Correl.* 1, 6, 10–39.

Póka T., Zelenka T., Szakács A., Seghedi I., Nagy G. & Simonits A. 1998: Petrology and geochemistry of the Miocene acidic explosive volcanism of the Bükk Foreland; Pannonian Basin, Hungary. *Acta Geol. Hung.* 41, 4, 437–466.

Püspöki Z., Makk-Tóth Á., Kozák M., Dávid Á., McIntosh R., Buday T., Demeter G., Kiss J., Terebesi-Püspöki M., Barta K., Csordás Cs. & Kiss J. 2009: Truncated higher order sequences as responses to compressive intraplate tectonic events on eustatic sea-level rise. *Sed. Geol.* 219, 208–236.

Radócz Gy. 1964: Geologische Untersuchungen im Braunkohlengebiet von Feketevölgy (Nord.Borsod). *Ann. Report Geol. Inst. Hungary from 1962*, 511–545.

Royden L.H. & Horváth F. 1988: The Pannonian basin — a study in basin evolution. *Amer. Assoc. Petrol. Geol. Mem*oir 45, 394.

Schréter Z. 1951: Berichte über die Geologischen untersuchungen in der umgebung von Bükkszék zwecks planmassinger anlage der erdölschürfungen. *Ann. Report Geol. Inst. Hungary from* 1945-47, 121–131.

Steininger F., Berggren D.V., Kent R.L., Bernor S., Sen S. & Agusti J. 1996: Circum-Mediterranean Neogene (Miocene–Pliocene) marine-continental chronologic correlations of European mammal units. In: Bernor R.L., Fahlbusch V. & Mittmann H.-W. (Eds.): The evolution of western Eurasian Neogene mammal faunas. *Columbia University Press*, New York, 7–46.

Szabó Cs., Harangi Sz. & Csontos L. 1992: Review of Neogene and Quaternary volcanism of the Carpathian-Pannonian region. *Tectonophysics* 208, 243–256.

Szakács A., Zelenka T., Márton E., Pécskay Z., Póka T. & Seghedi I. 1998: Miocene acidic explosive volcanism in the Bükk Foreland, Hungary: Identifying eruptive sequences and searching for source locations. *Acta Geol. Hung.* 41, 4, 429–451.

Sztanó O. & Józsa S. 1996: Interaction of basin-margin faults and tidal currents on nearshore sedimentary architecture and composition: a case study from the early Miocene of Northern Hungary. *Tectonophysics* 266, 319–341.

Sztanó O. & Tari G. 1993: Early Miocene basin evolution in Northern Hungary: Tectonics and Eustacy. *Tectonophysics* 226, 485–502.

Sztanó O., Szafián P., Magyar I., Horányi A., Bada G., Hughes D.W., Hoyer D.L. & Wallis R.J. 2013: Aggradation and progradation controlled clinothems and deep-water sand delivery model in the Neogene Lake Pannon, Makó Trough, Pannonian Basin, SE Hungary. *Global Planet. Change* 103, 149–167.

Tari G. 1988: Strike-slip origin of the Vatta-Maklár trough. *Acta Geol. Hung.* 31, 101–109.

Tari G., Báldi T. & Báldi-Beke M. 1993: Paleogene retroarc flexural basin beneath the Neogene Pannonian Basin: a geodynamic model. *Tectonophysics* 226, 433–455.

Telegdi-Róth K. 1951: Enseignements Geologiques de la prospection et de la productions du pétrole a Bükkszék. *Annals Geol. Inst. Hungary*, 40, 2, 1–21.